HABILITATION À DIRIGER DES RECHERCHES

Spécialité : **Sciences de la Terre**

Présentée par

Mai-Linh DOAN

préparée au sein d' **ISTerre**
et de l'**Ecole Doctorale Terre, Univers, Environnement**

Localization processes within active faults
Insights from high strain rate experiments and in-situ characterization

Thèse soutenue publiquement le **20 novembre 2013**,
devant le jury composé de :

M., Georg DRESEN
GFZ Postdam, Germany, Rapporteur
M., Daniel FAULKNER
Liverpool University, United Kingdom, Rapporteur
M.,Yves GUGLIELMI
Université Aix-Marseille / CEREGE, France, Rapporteur
M., Fabrice COTTON
Université Grenoble Alpes, France, Examinateur
M., Jean CHERY
Université de Montpellier II, France, Examinateur

Contents

Chapter 0

Résumé étendu en français

La mécanique des failles actives est une science jeune. Une question en apparence aussi simples que la structure des failles actives est encore une question ouverte. La structure fine d'une faille active est en effet difficile à prédire *a priori*. Or cette structuration est un pré-requis pour comprendre la mécanique d'une faille active, des processus de nucléation présismiques, des processus de propagation du glissement cosismiques, ou encore des processus de recimentation postsismiques.

Sur le terrain, les failles présentent différentes structures. Certaines peuvent se présenter comme une faille simple, où la déformation est localisée dans un cœur de faille entouré d'une zone endommagée. D'autres sont plus complexes, avec plusieurs zones localisant le glissement. Cette structuration est le reflet d'interactions entre les processus d'initiation du glissement, d'endommagement et de recimentation.

Mes travaux traitent des processus de localisation dans des failles actives, par une approche multi-échelle. De l'échelle métrique à décamétrique, les données en forage permettent d'avoir un profil continu des propriétés physiques à travers une faille. Les forages permettent aussi l'installation d'observatoires long terme. A l'échelle centimétrique, les expériences de laboratoire permettent d'identifier et de caractériser les processus contrôlant l'évolution de l'endommagement et de la localisation de la déformation.

0.1 Résumé des travaux

0.1.1 Caractérisation in-situ des failles actives

Durant la dernière décennie, plusieurs forages ont été entrepris pour caractériser les failles actives en profondeur. Forer apporte plusieurs informations inaccessibles autrement: il est possible (1) d'obtenir des échantillons frais, sans altération, (2) de caractériser la structure et les propriétés des failles dans des conditions de température et de contraintes in-situ, de l'échelle décimétrique à décamétrique (3) d'installer des observatoires permanents pour suivre au plus près l'évolution des failles au cours du cycle sismique. Au cours de mon activité de recherche, j'ai pu couvrir tous ces aspects.

Processus de fluage au sein de la faille de San Andreas

Lors de la thèse de Julie Richard, co-encadrée avec Jean-Pierre Gratier, j'ai pu observer des échantillons récoltés dans le forage SAFOD (San Andreas Fault Observatory at Depth).

Dans la zone endommagée entourant le cœur de de faille, on peut observer des traces importantes de dissolution-cristallisation [*Gratier et al.*, 2011]. Ce processus est activé par la microfracturation intense des grains, dont on ne peut écarter une origine dynamique [*Doan and Gary*, 2009].

Dans la zone de faille, la déformation est accommodée par des phyllosilicates de friction très faible, qui présente de multiples zone de localisation le long de nombreuses structures S-C. La dissolution-cristallisation reste toutefois importante [*Richard et al.*, 2014a].

Caractérisation in situ des propriétés hydrauliques des failles

Les forages permettent d'accéder aux roches de failles en condition in-situ. Les mesures réalisées ne sont donc pas biaisées par d'éventuelles décompressions ou de changement de géochimie des fluides interstitiels. C'est donc une méthode de choix pour caractériser les propriétés hydromécaniques du milieu.

Quasi systématiquement, des diagraphies en forage sont réalisées. Elles permettent d'obtenir des profils continus des propriétés physiques des roches en place, comme la résistivité électrique des roches, les vitesses des ondes sismiques ou l'émission radioactive naturelle. Indirectement, elles permettent d'accéder à la porosité des roches (par exemple *Doan et al.* [2011]). Elles permettent aussi d'inférer un profil continu de perméabilité, au moins qualitatif [*Saffer et al.*, 2013; *Doan et al.*, a], ce qui permettrait de caractériser l'extension de la zone endommagée d'une faille.

Ces données sont couplées à des mesures hydrauliques directes par essai de pompage. Ces méthodes sont assez couteuses et ponctuelles, mais donnent des mesures fiables. Une première méthode consiste à immerger une pompe et tester un large intervalle du puits: cette méthode est peu précise spatialement mais elle permet d'étudier un large volume si le pompage est suffisamment long. Par exemple, *Doan et al.* [2006a] ont pu mesurer la perméabilité de la zone endommagée de la faille de Chelungpu, à l'origine du séisme de Chichi en 1999. Cet essai par choc hydraulique été mesuré sur 2 semaines. La faible diffusivité hydraulique mesurée ($\sim 7 \times 10^{-5}\,\mathrm{m^2/s}$) rendrait plus efficace l'adoucissement de la faille par pressurisation thermique.

Une autre méthode consiste à utiliser une sonde spécifique, comme le MDT (Modular formation Dynamics Tester) de Schlumberger. Cet outil issu de l'industrie pétrolière permet d'effectuer des essais hydrauliques sur des sections de forage isolées par des obturateurs. Les essais peuvent être réalisés à l'échelle centimétrique ou métrique. Le coût est très élevé, et l'outil demande un puits de bonne qualité et de grand diamètre. Son premier déploiement dans le cadre d'IODP (International Oceanic Drilling Program) n'a donc pu se faire que lors de la mission IODP 319 [*Moe et al.*, 2012], qui a été la première à utiliser la technologie riser dans le cadre du programme NanTroSEIZE (Nankai Trough SEImic Zone Experiment). Grâce à cet outil, on a pu obtenir une perméabilité in-situ à l'échelle métrique et centimétrique [*Boutt et al.*, 2012], et estimer des profils de pression de pore [*Saffer et al.*, 2013] et de contraintes [*Ito et al.*, 2013].

Suivi long terme de l'évolution de la pression interstitielle

L'installation d'un observatoire permet de suivre l'évolution de la faille au cours du temps. Même en dehors du cycle sismique, les failles peuvent subir des variations importantes de pression. Par exemple, lors de ma thèse [*Doan*, 2005], j'avais pu observer que la pression de pore mesurée près de la faille d'Aigion chutait au passage des ondes télésismiques générées par un séisme d'épicentre éloigné de plus 10 000 km [*Doan and Cornet*, 2007].

Le dépouillement des données demande un filtrage des marées terrestres et des fluctuations barométriques. La réponse à ces forçages renseignent indirectement sur les propriétés hydromécaniques du milieu [*Doan et al.*, 2006b].

L'accès à ces données est difficile, car peu d'observatoires ont été installés dans des failles actives. Cette activité se fait en collaboration. J'ai pu ainsi accéder aux données de pression acquises par l'instrumentation installée dans phase 1 du projet Deep Fault Drilling Project, qui étudie la faille de San Andreas.

0.1.2 Étude en laboratoire de la localisation dynamique de l'endommagement

En marge de mes activités de forage, au potentiel scientifique important, mais de nature épisodique, je me suis consacrée à des expériences de mécanique des roches en laboratoire. Ces études concernent aussi la problématique de la localisation de la déformation lors d'un séisme, que ce soit dans la zone endommagée cernant la zone de faille, ou dans le cœur de faille.

Inhibition de la localisation lors de l'endommagement dynamique des roches

Les vitesses de glissement cosismiques atteignent le mètre par seconde, voire la dizaine de mètre par seconde. De plus, les vitesses de propagation du glissement sont proches des vitesses des ondes dans le milieu. On entre dans le domaine de la mécanique de la fracture dynamique.

Les effets inertiels deviennent alors non négligeables [*Grady and Kipp*, 1987]: la vitesse de propagation des fractures au sein du milieu devient limitée par la vitesse des ondes sismiques [*Bhat et al.*, 2012]. Les temps caractéristiques d'interaction entre fractures deviennent similaires à ceux de la propagation des fractures les plus favorables [*Denoual and Hild*, 2000]. On s'attend donc à la propagation simultanées de plusieurs fractures et à la multifragmentation du milieu, comme ce qui est observé près des zones d'impact de météorite [*Melosh*, 1989].

Curieusement, l'étude de l'endommagement dynamique a été délaissée jusque vers le milieu des années 2000. Mes études ont été motivées par la découverte de roches pulvérisées [*Wilson et al.*, 2005; *Dor et al.*, 2006] près des zones de failles. Ces roches sont finement fragmentées mais restent peu déformées. Elles s'étendent de manière continue plusieurs centaines de mètres autour du cœur de faille. Tout se passe comme si la déformation restait diffuse au lieu de se localiser le long de grandes fractures, comme observé à cette distance du cœur de faille. Cet endommagement rappelle l'endommagement dynamique des roches.

Pour tester l'origine dynamique des roches pulvérisées, j'ai testé des échantillons de roches prélevées près du segment Mojave de la faille de San Andreas sur un banc de barres de Hopkinson. Avec un tel dispositif, on peut obtenir des courbes contraintes-déformation jusque des vitesses de déformation de plusieurs milliers par seconde. Les expériences ont permis de reproduire un endommagement proche de la pulvérisation [*Doan and Gary*, 2009]. On observe en effet macroscopiquement trois états finaux pour les échantillons: soit les échantillons restent intacts, soit les échantillons sont fendus en 2 ou 3 fragments, soit les échantillons sont finement multifragmentés. La transition semble contrôlée par la vitesse de déformation, plutôt que par la déformation ou par le confinement dynamique. Cette observation a été renouvelée sur d'autres roches cristallines [*Yuan et al.*, 2011; *Doan and D'Hour*, 2012]. Par contre, des expériences sur des marbres ne permettent pas de retrouver une pulvérisation à haute vitesse de déformation et faible déformation [*Doan and Billi*, 2011]. Ceci est cohérent avec l'absence de roches pulvérisées trouvées dans les roches carbonatées [*Dor et al.*, 2006]. Le seuil en vitesse de déformation est contrôlée par la distribution statistique de défauts dans le milieu. Notamment, le seuil est abaissé pour une roche très endommagée. Des chargements multiples au cours de plusieurs cycles sismiques contribuent à une fracturation plus fine des roches pulvérisées près du cœur de failles.

Dans une deuxième étape, j'ai collaboré avec des géologues structuraux pour caractériser l'endommagement dynamique. Les échantillons ont été chargés en deçà du seuil de rupture de façon à obtenir des échantillons préservés, dont les propriétés physiques peuvent être étudiées. Ces études ont révélé que les échantillons sont finement microfracturés, ce qui induit une diminution de la vitesse sismique des ces ondes [*Doan et al.*, 2009], et surtout une augmentation substantielle de la perméabilité de ces roches. Les microstructures observées et les perméabilités mesurées sont proches de celle mesurées sur des échantillons prélevés près de la faille de San Jacinto [*Mitchell et al.*, 2013].

Influence des impuretés de talc sur l'initiation du glissement dynamique de la serpentine

Avec des collègues grenoblois et lyonnais, nous avons lancé une étude sur la friction à vitesse cosismique du talc et de la serpentine. Cette étude a été lancée en 2008, au moment où du talc a été découvert dans des fragments extraits du forage SAFOD [*Moore and Rymer*, 2007]. Le talc est connu son faible coefficient de friction, et il a été soupçonné de lubrifier la faille de San Andreas. Comme le talc est issu de la décomposition de pyroxène en milieu saturé de silice, son association avec la serpentine est attendue dans des failles sismiques, comme les failles de subduction.

L'étude a d'abord consisté en l'étude du talc seul, dont les propriétés de friction à haute vitesse de cisaillement n'avaient pas été étudiées jusque là [*Boutareaud et al.*, 2012]. Nous avons montré que

le talc sec avait une forte friction initiale, beaucoup plus importante que le talc à faible vitesse de déformation. Au contraire, le talc humide ne présente pas de pic initial de friction, comme ce qui a été observé pour d'autres phyllosilicates [*Faulkner et al.*, 2011]. L'humidité altère aussi la localisation de la déformation dans l'échantillon.

La suite de l'étude a consisté en l'étude de la friction de mélanges de talc et de serpentine [*Doan et al.*, b]. En conditions humides, où le talc est un matériau faible, le talc altère la friction initiale dès des concentrations de 5% de talc. Les microstructures observées sont beaucoup plus diffuses que dans le cas de la serpentine pure, avec une déformation répartie sur l'ensemble de la gouge, initiée sur les grains de talc en cours de délamination, qui servent à microlocaliser le glissement.

Dans ces deux études, la localisation du glissement est fortement dépendante de la proportion de microdéfauts susceptibles de localiser la déformation. Dans les deux cas, en cas de chargement rapide, la localisation de la déformation peut être inhibée.

0.2 Perspectives

0.2.1 S'approcher des conditions sismogéniques

Les forages traversant les failles actives tendent à viser des profondeurs de plus en plus importantes (table 4.1). On aborde alors des contraintes et des températures plus élevées. Ces conditions activent des processus de fluage, soit par pression-solution, soit par activation de la plasticité des minéraux. Les processus que j'ai étudiés jusqu'à présent relevaient surtout du domaine fragile. A moyen terme, je compte m'approcher de conditions plus ductiles, et ce pour les deux approches expérimentales et in-situ.

L'activité en forage est une activité fortement épisodique, du fait du faible nombre de forages internationaux en cours. J'ai cependant été amenée à participer à plusieurs workshops d'avant projet concernant des forages traversant des failles actives:

- La faille Alpine en Nouvelle-Zélande a une composante inverse qui fait remonter des matériaux ductile. Elle induit aussi une anomalie thermique. On peut donc étudier par des forages de profondeur modérée des processus ductiles. Je suis partie prenante de la phase 2 du projet qui vise à forer et instrumenter la faille à près de 1500 m de profondeur.
- Le projet NantroSEIZE vise à percer le décollement de la zone de subduction de Nankai. Il est prévu de prolonger le puits C002 jusqu'à intercepter ce décollement à 7000 m de profondeur
- Le projet Japan Beyond Brittle Project est un projet de géothermie profonde, visant à faire circuler des fluides à haute enthalpie dans des matériaux ductiles. Bien que le projet ne vise pas des failles actives préexistantes en particulier, il approche des thématiques liées, comme le suivi microsismique et la vitesse de recimentation des fractures. J'ai été invité à participer au workshop ICDP préliminaire en mars 2013.

0.2.2 Réunir les approches expérimentales et in-situ

Les travaux réalisés jusqu'à présent concernaient surtout l'endommagement des matériaux fragiles. Le lien entre expériences en laboratoire et les travaux en forage restent encore ténu. Le verrou principal est l'absence de fort confinement des expériences en laboratoire. A cela s'ajoute la faible saturation en eau des roches. L'arrivée à Grenoble de Pascal Forquin va permettre de développer ces aspects par des essais œdométriques d'échantillons saturés.

Pour les travaux de pulvérisation, il est important de mieux caractériser l'endommagement. Pour cela, nous envisageons d'utiliser un surfacemètre BET, en voie d'acquisition à ISTerre.

La création d'un réseau microfracturé va altérer la circulation de fluide. La faible distance interfracture est notamment suspecté d'activer les processus de recimentation et fluage des failles par pression-solution. Nous comptons donc effectuer des expériences de percolation sous contrainte pour étudier ces processus. Ces travaux initiés lors de la thèse de Julie Richard seront poursuivis lors de la thèse de Frans Aben.

Chapter 1

Introduction

Predicting earthquakes is the Graal of seismologists, a dream so far not realized. Major faults can experience precursory activity [*Bouchon et al.*, 2011], as monitored from seismic network. However, surface observations failed to provide systematic precursors prior to an earthquake, even when an extensive network of instruments has been deployed, like at Parkfield, California [*Johnston et al.*, 2006]. A major obstacle to predictability of the behavior of active faults is their structural complexity.

Let illustrate this complexity with the San Andreas Fault Observatory at Depth (SAFOD) project, that was drilled through the San Andreas Fault, deeper than 3 km (figure 1.1). The project is one of the greatest recent achievements in fault drilling and provided many outcomes: it showed that the creep behavior could be better explained by the weak friction coefficient of the saponite, a subproduct of alteration [*Lockner et al.*, 2011] or by pressure-solution process [*Gratier et al.*, 2011], but certainly not by high fluid pressure [*Rice*, 1992].

It provided also many surprises. The fault was not separating the crystalline Salinian formation from the Fransciscan mélange: instead, unexpected arkosic sandstone laid on the western side of the fault. The fault itself is much thicker than the simple planar structures envisioned by seismologist and geodesist, with a damage zone more than 200 m wide. Within this fault core, two major deformation zones were able to twist the metallic casing of the hole. Several observations don't match the standard pictures described by structural geologists [*Chester and Logan*, 1986]: cores did not show principal shear zone localizing deformation within few centimeters, as seen for instance within the Chelungpu fault [*Ma et al.*, 2006], whereas the damage zone stops abruptly on one of the deformation zone.

Note also how the authors of figure 1.1 try to connect the two major deformation zone seen in the SAFOD borehole to the microseismic swarm found about 100 m away from the borehole. Given the errors in event locations, it is a bit audacious. This illustrates the major challenge towards predictive fault mechanics: it is difficult to extrapolate the structures observed outside the range of observation.

This difficulty in structure predictability is annoying, since the structure of a fault affects several properties:

– Their propensity to fail. The gouge of last slipping strand can be substantially weak, but it is also consolidated by healing, sometimes becoming stronger than prior to slip. Healing of this zone depends on the fluid geochemistry, that can be changed by enhanced permeability along fault (fault valve effect, [*Sibson*, 1992]). Pressure solution is also enhanced by smaller grain size, that can be due to co-seismic fragmentation [*Doan and Gary*, 2009], and the presence in moderate amount of clays [*Bos et al.*, 2000].

– Their transport properties, as permeability varies as the cube of the fracture aperture. It is often seen that fractures are found along not in the core itself (because gouges are often plastic, full of clay), but in the nearby damage zone (large fractures take a longer time to heal [*Gratier and Gueydan*, 2007; *Gratier et al.*, 2011]).
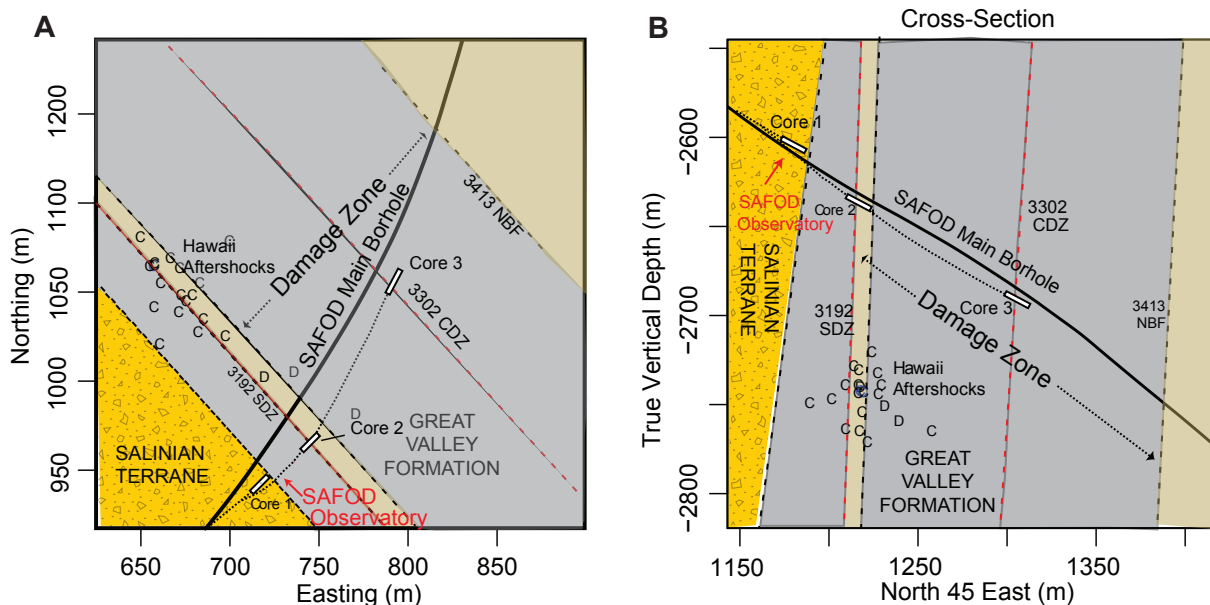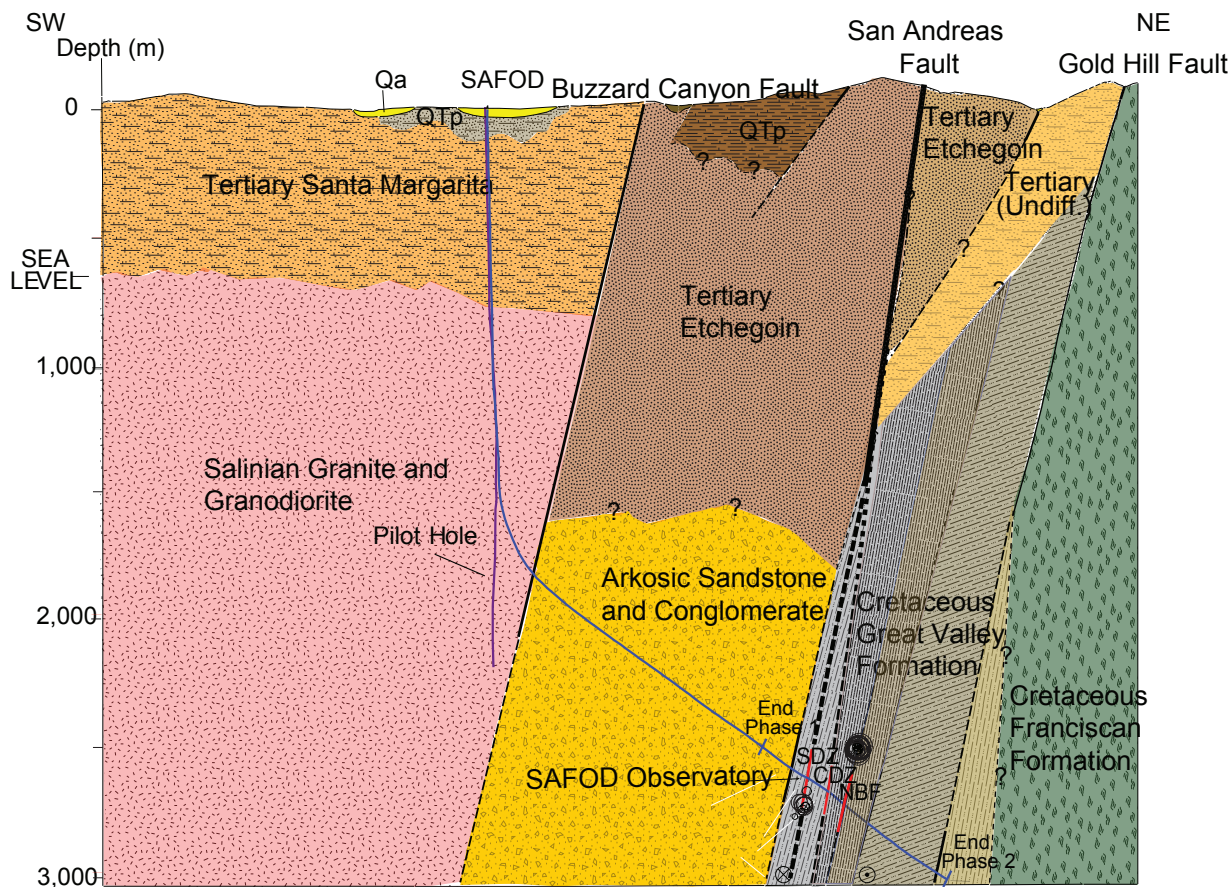
Figure 1.1: Cross section of the SAFOD boreholes. The 2 close-up at the bottom zooms on the borehole trajectory within the San Andreas Fault (lower left: map view, lower right: cross section, zoom from the above figure). From *Zoback et al.* [2011].

– Their mechanical compliance, not only because of the presence of weak components like clay, but because the large amount of fractures within the damage zone. Mechanical compliance may control the sensitivity of fault to static triggering by nearby earthquakes or dynamic triggering by teleseismic waves.

How to improve our knowledge on fault structure ?

A first approach is by observing more natural faults, and trying to identify several typical structures.Natural active faults have a variety of structures [*Faulkner et al.*, 2010; *Caine et al.*, 1996]. They can be composed of a single very localized strand [*Chester and Logan*, 1986] or be formed of a series of anastamosing fault surfaces [*Faulkner et al.*, 2003] that isolate strong lenses within a fault [*Candela and Renard*, 2012]. These structures can be described by the variation of the physical parameters, which can be quantified and characterized at several scales.

I performed such a quantification using geophysical data from boreholes drilled through active faults. Boreholes provide exceptional opportunities to understand fault structures in in-situ conditons and monitor fault evolution at depth. Using such data, I could provide and help refining models describing profiles of permeability across several major active faults (Chelungpu Fault, San Andreas Fault, Nankai Trough). From long term monitoring, I could show how these parameters can vary through time.

A second approach is by performing laboratory experiments to reproduce these structures, and identifying and explaining how a fault gets structured. Scale there is centimetric, much smaller than the field scale observation. Hence I redesigned the experiments to understand the more general question of strain localization, and how it is controlled by strain rate. I especially discuss the high strain rate processes, that are expected to occur during slip, or even at the arrival of the seismic waves of the approaching rupture patch, and how they prepare the fault prior to its slip. In particular, I focus on high strain rate damage. I also worked on the dynamic structuration of a fault gouge during high velocity shearing, using a technique that revolutionized friction studies [*Di Toro et al.*, 2011].

The report is structured from small-scale process to large scale processes, from the sub-centimetric fault core which localized slip to the decameteric structure of the damage zone.

– We start from the center of the fault, with high velocity friction experiments on mixture of talc and serpentine, at the millimetric scale. At high velocity, structure and friction interplay. Especially, small amount of talc help localizing deformation along many small shear planes, thus limiting strain concentration on the principal shear zone at the edge of the sample. Minor changes in gouge composition can change the width of the shear zone, or alter the easiness a creation of new shear zone. This is bad omen for predicting fault structure.

– We then discuss high strain rate fragmentation in the damage zone, at the centrimetric scale. I pioneered the application of high strain damage experiments to fault mechanics, to understand pulverized rocks, a damage feature recently discovered [*Dor et al.*, 2006]. I showed that high strain rate inhibit strain localization. Therefore, pulverized rocks might be related to coseismic damage, and that they could be marker of previous large earthquakes [*Doan and Gary*, 2009]. Pulverization can also change permeability drastically [*Mitchell et al.*, 2013], showing that fault structure is time-dependent.

– We finish with borehole studies in active faults. I show how it is possible to get continuous profiles of permeability and porosity to characterize damage extent around faults [*Doan et al.*, 2011, a] at the decametric scale. I also discuss how long term pore pressure monitoring could monitor fault destabilisation either from teleseismic waves, or even prior a major fault disturbance.

Chapter 2

Localization process at the onset of coseismic slip

In this section, we will discuss the behavior of fault gouge at the millimetric scale to understand how a mixture of weak and strong material behaves at high sliding velocities. Such high velocity friction experiments revolutionized our knowledge of fault friction, by showing dramatic reduction in friction properties [*Di Toro et al.*, 2011], through many processes, often thermally activated (thermal pressurization [*Wibberley and Shimamoto*, 2005], phase transitions like decarbonatation [*Han et al.*, 2010], melting [*Hirose*, 2005],...).

For usual friction experiments, inserting material of weak friction randomly in a mixture is not very effective, as large concentrations are needed to reduce the effective friction of the mixture (eg, see the 50%-50% results for mixture of talc and quartz by *Carpenter et al.* [2009]). The mixture needs to be structured to change the friction, with the constitution of a continuous layer of weak material [*Niemeijer et al.*, 2010; *Moore and Lockner*, 2011]. Are weak heterogeneities more efficient at high sliding velocity ?

Together with Takehiro Hirose, Sébastien Boutareaud, Muriel Andréani and Anne-Marie Boullier, I conducted high velocity friction experiments on mixtures of gouge and talc. This mixture is pertinent geologically, since talc is a product of alteration of pyroxene is silica-rich environment and is often associated with serpentine in ultramafic rocks. The layers of this phyllosilicate slide easily also their basal direction, so that is friction is very small (about 0.15 [*Moore and Rymer*, 2007], much less than the 0.6-0.8 range found for most material [*Byerlee*, 1978]) . Such combination are expected to occur in along faults bordering core-complexes at mid-ocean ridges [*Ildefonse et al.*, 2007], subduction zones [*Manning*, 1995]. We launched the project at the time when talc fragments were identified within the SAFOD borehole [*Moore and Rymer*, 2007]. Given its very low friction coefficient, it was suspected to lubricate the San Andreas Fault.

2.1 Water dependence of talc friction at high strain rate

We first investigated the high velocity friction behavior of talc, in both saturated and unsaturated conditions, since at that time its properties at high velocity friction experiments were not characterized.

Figure 2.1 shows that unsaturated talc exhibits very large friction compared to slow slip rate conditions. Figure 2.2 shows the associated microstructures seen with Scanning Electron Microscopy (SEM). A S-C structure pervades the center of the rouge, so that most of the grains are not favorably oriented to accommodate the formation. At the boundary with the rotating cylinder driving the sample rotation, a principal slip zone (PSZ) seems to accommodate the deformation: it is finely comminuted, with some remnants of layers of talc parallel to the shear direction. Transmission Electron Microscopy (TEM) on the PSZ shows that talc has been finely delaminated and advected by the rotational movement to form nanometric aggregates (figure 2.3). It is probable that the peak
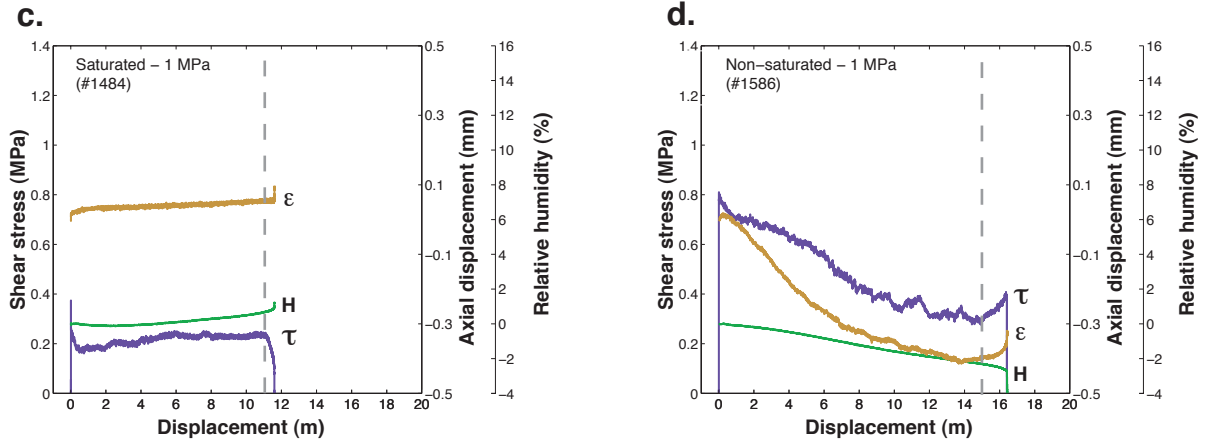
Figure 2.1: Evolution of friction coefficient with displacement for water saturated talc (left graph) and dry talc (right graph). From *Boutareaud et al.* [2012].

in friction is cause by jamming of the talc particles, that was resolved within the PSZ by intense delamination.

The experimental curves obtained for wet talc give lower friction, closer to the slow strain rate results, once friction induced by friction on the teflon ring holding the artificial gouge has been removed. Almost from the onset of slip, talc friction is small. The effect of water can be multiple: it can be related either to thermal pressurization, as for other wet phyllosilicate gouges [*Faulkner et al.*, 2011], or to hydrodynamic lubrication at the boundary of the hydrophobic talc layers, that facilitates the rotation of talc grains to the most favorable angle, parallel to the shear direction.

2.2 Effect of small amount of talc on the onset of friction of gouges of serpentine and talc

To tackle the friction properties of serpentine and talc, we kept saturated conditions, where talc has low friction coefficient, and can be considered as the weak component of the gouge mixture. Several mixtures of various proportions were tested. For these experiments, we used a loose Teflon ring of standardized dimension to limit its effect on friction. To assess the effect of the Teflon sleeve on the recorded friction experiments, we performed dummy tests, with only the Teflon ring and water inside the ring. The Teflon effect is reproducible and negligible: the shear stress due to friction on Teflon ring is 0.03 MPa.

The experiments in wet conditions show a spectacular weakening effect of talc on the mixture (figure 2.4). Pure serpentine experiences strong slip weakening, with a peak friction coefficient of 0.5 that falls exponentially to a steady-state value of 0.2 with a characteristic slip-weakening distance D_c of 7 m. Talc has a very different behavior: it begins to slide without a sharp friction peak and keeps nearly constant friction coefficient of 0.2-0.25. Adding more than 5%wt talc levels off the initial peak in friction and initial friction is reduced to 0.37. Friction levels to this value before rejoining the decay curve of pure serpentine after 3 m of slip.

The two gouge components have very different behaviors (figure 2.3, left). Serpentine tends to break into angular fragments. Hence, pure serpentine gouge tends to form PSZ finely comminuted (figure 2.5, A). On the contrary, talc tends to kink and delaminate easily. The insertion of talc seems to reduce the extent of the principal shear zone. Meanwhile within the center of the gouge, several shear zones appear, creating a flowing structures. The small shear fractures follow alignment of talc grains that delaminated (figure 2.5, F).

A possible scenario is that peak in friction is related to jamming of serpentine grains that was resolved by the abrasion of serpentine grains and possibly thermal pressurization. Introducing talc,
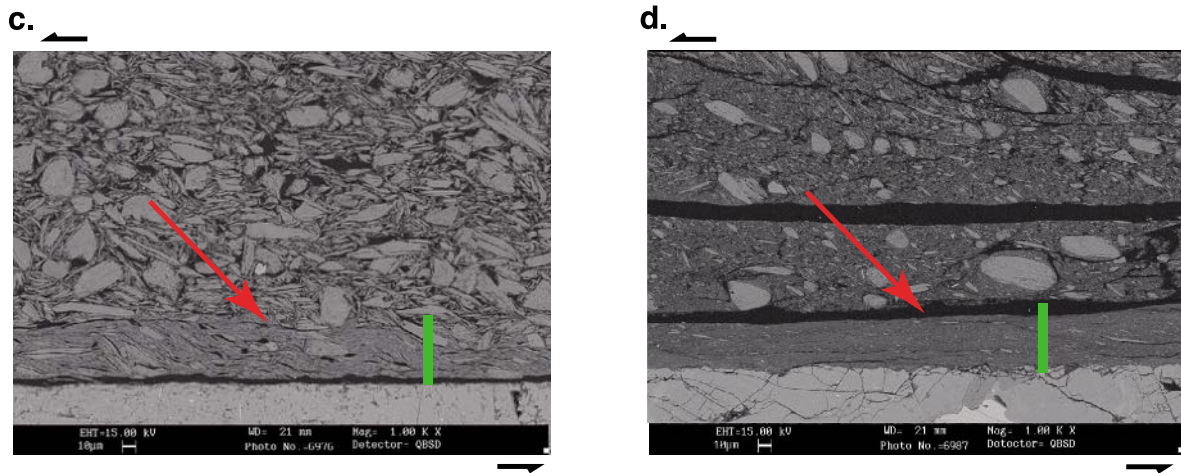
11

Figure 2.2: Microstructures of the principal slip zones (PSZ) generated during the experiments shown on figure 2.1. (Left) SEM backscattered images in wet conditions, the PSZ contains talc lamellae of large dimensions; entangled in a tight S-C structure. The top of the image shows the that in the less disturbed center of the gouge, talc grains get oriented parallel to the slip direction, in a direction favorable for a basal slip. (Right) SEM backscattered image in dry conditions. The center of the gouge show the tip of the S-C structure pervading the center of the gouge, where most of the grains are not orientated favorably for S-C sliding .From *Boutareaud et al.* [2012].
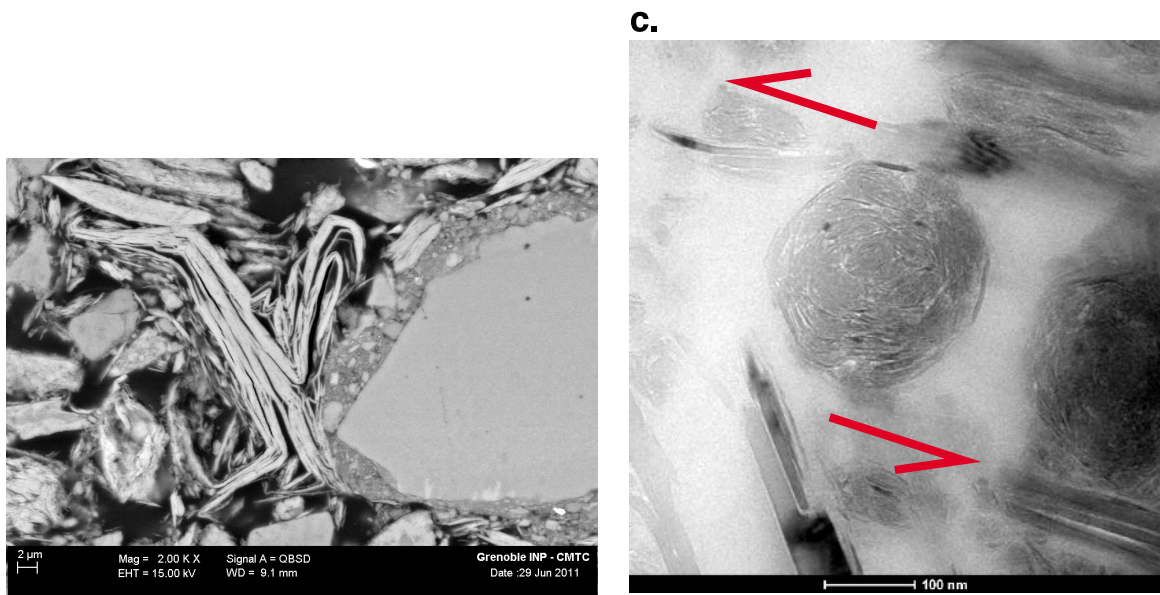

Figure 2.3: Microstructural image showing easy talc delamination. (Left) SEM photograph showing the easy delamination of talc compared, whereas serpentine grains tend to break into angular fragments. (Right) TEM photograph, where extremely delaminated talc was rolled to nanometric aggregate (from *Boutareaud et al.* [2012]).
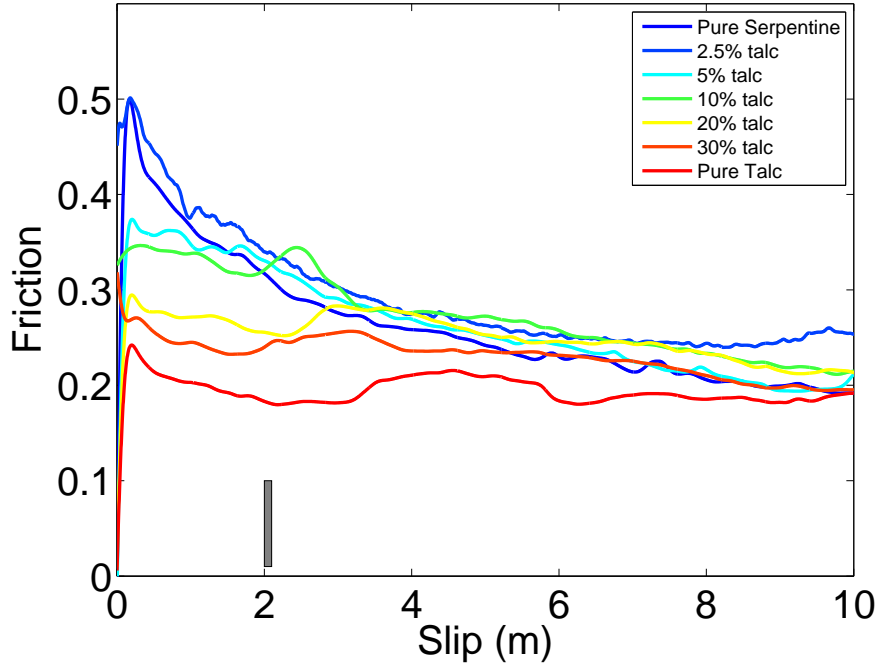
Figure 2.4: Evolution of friction coefficient with displacement for wet mixtures of serpentine and talc. Talc concentration as small as 5%wt is enough to reduce the initial peak in friction. From *Doan et al.* [b]

eased the formation of local shear zone, that helped overcome the grain-to-grain interlocking of serpentine.

2.3 Conclusions

In this section, we showed that the dynamic properties of friction were quite different from the low strain rate properties. For instance, jamming of dry talc prevented the reorientation of talc grains into a favorable angle and gave large friction coefficients. Similar happens for serpentine gouge alone.

The softening process seems to be eased by "strain catalysts". For wet talc, water seems to favor the reorientation of talc into a favorable sliding direction. For mixtures of talc and serpentine, delamination of talc grains initiate small shear zone, creating a more diffuse pattern of strain than for serpentine. This effect occurs from the onset of friction. The reduction of the initial peak in friction has several important implication for rupture propagation [*Faulkner et al.*, 2011]: it reduces the frictional strength of the fault zone and the neutral frictional behavior would make talc-rich zones, neither seismogenic, since there no slip weakening, neither barrier to further earthquake rupture since there is not slip strengthening.
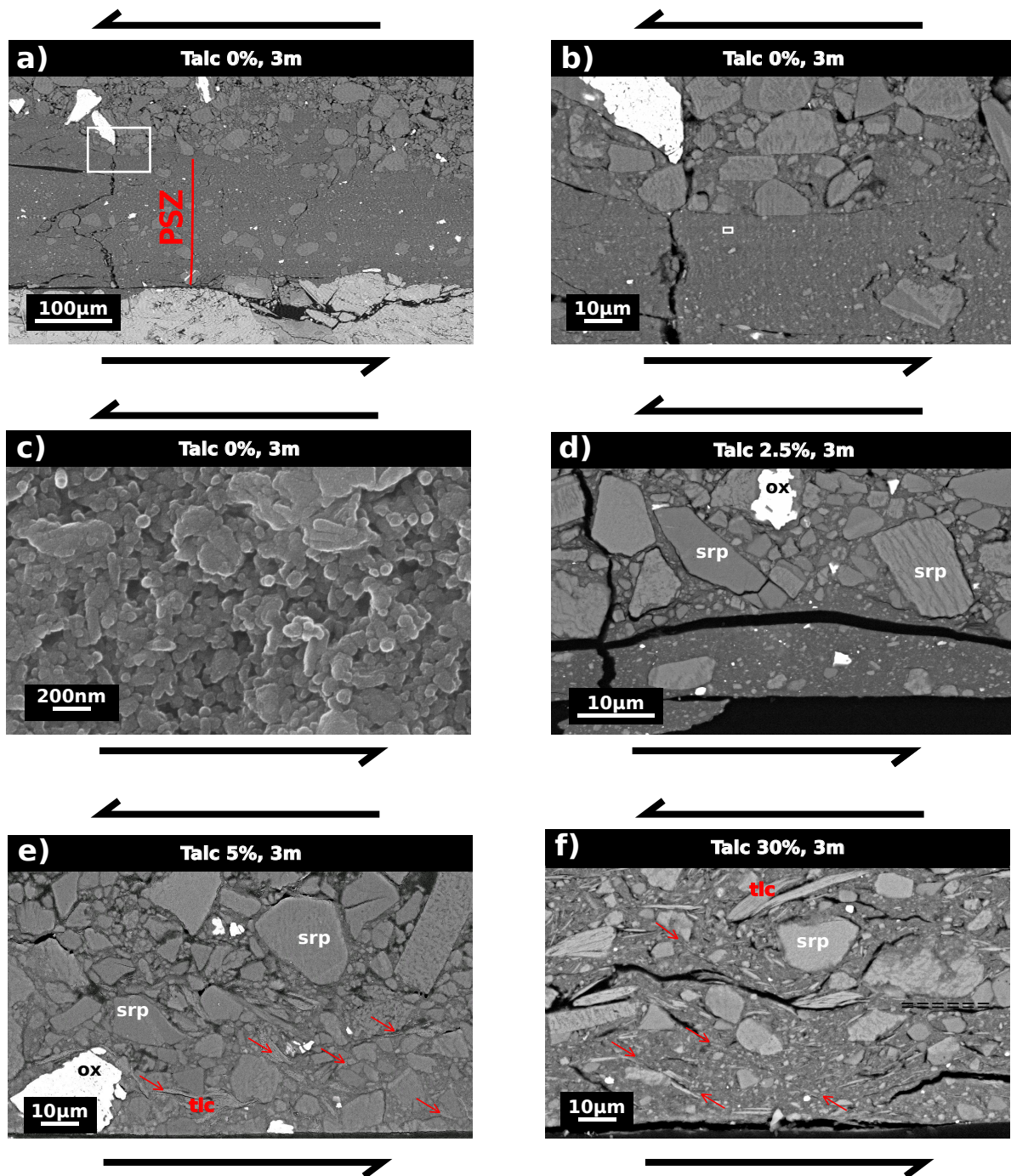
Figure 2.5: Microstructure of the sliding zone after 3 m of slip observed with a FE SEM. (A) Pure serpentinite with a 100 μm-wide Principal Shear Zone (PSZ). White grains are magnetite (iron oxyde). (B) Focus on the sharp boundary between the PSZ and the main gouge. (C) Zoom on the submicron grain constituting the PSZ matrix. (D) Mixture with 2.5%wt talc. The PSZ is thinner but the texture is still similar to the pure serpentinite case. On this photograph, the heterogeneous color contrast of the serpentinite grains is due to the fact that serpentinite grains are aggregates of small crystals. (E) Mixture with 5% talc. Comminution of serpentine grains within the PSZ is reduced. Grains of talc coat the serpentine grains (red arrows). (F) Mixture with 30%wt talc. There is no developed PSZ, but there are many shear planes characterized by alignment of talc grains (red arrows). From *Doan et al.* [b].

Chapter 3

Damage localization during an earthquake

Fault localizes slip within a narrow core filled by fine-grained material named gouge. Around this core, lies a damage zone of variable extension, with decreasing fracture density with distance from the core. Damage near fault can be generated by several processes [Mitchell and Faulkner, 2009], either statically from the slow extension of the fault, or dynamically during the rupture process.
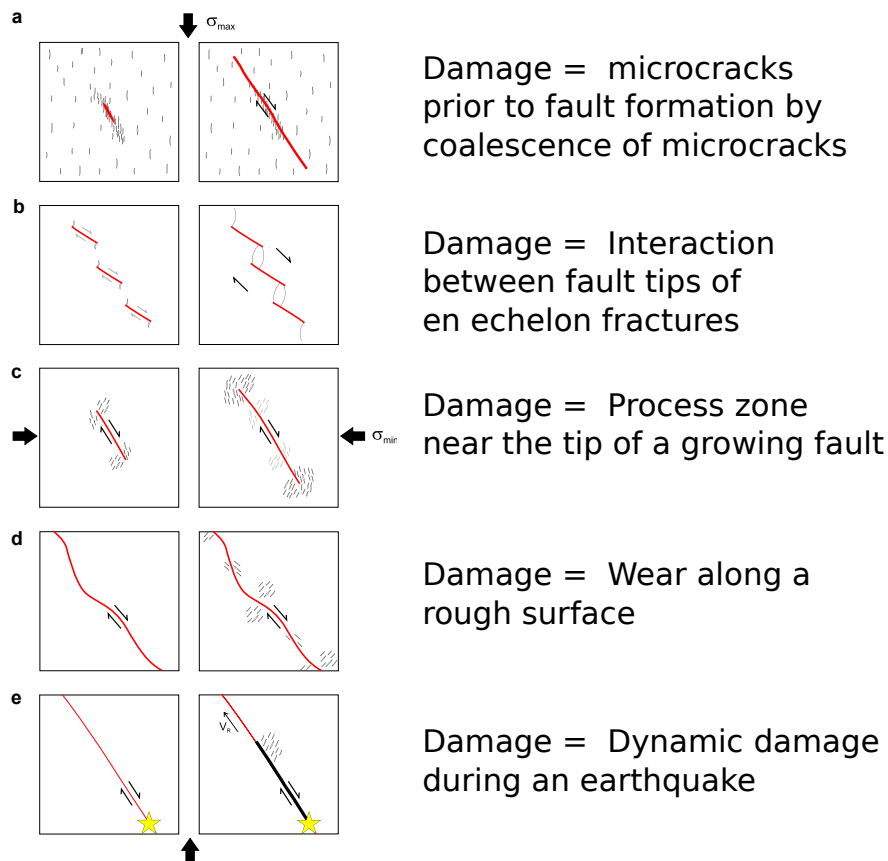
Figure 3.1: Review of 5 models explaining the damage observed around faults. Dynamic damage (model e) would be overprinted with other mechanisms of damage and subsequent fault healing. From *Mitchell and Faulkner* [2009].

Deciphering dynamic damage is difficult because of the overprinting of static damage, inherited during the maturation of the fault, and the subsequent healing. The best location to assess the extent of dynamic damage is a shallow environment – where healing is slow [*Gratier*, 2011] –, near
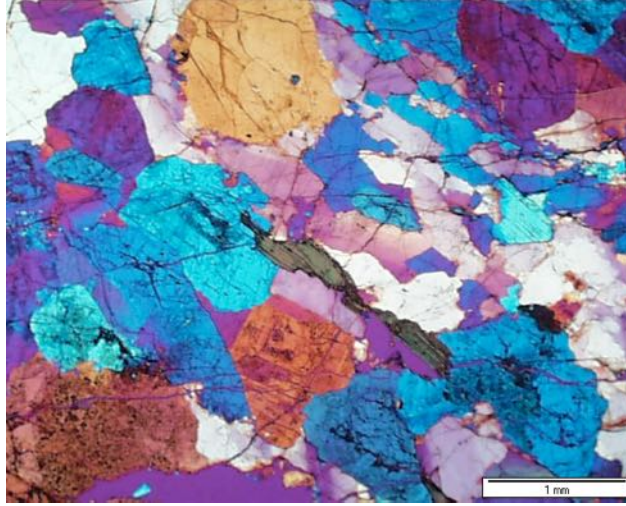
Figure 3.2: Thin section of a pulverized rock sampled near Lake Hughes, along the Mojave segment of the San Andreas Fault. The sample is microfractures, with fractures cutting through grains. The initial grain structure is preserved. Feldspar alteration is present but cannot explain the weakness of the rock. From *Doan and D'Hour* [2012]

3.1 Pulverization: an extreme case of dynamic damage

Pulverized rocks is a peculiar form of damage, only recently identified, first near major Californian faults [*Wilson et al.*, 2005; *Dor et al.*, 2006], and observed thereafter on several active faults (Northern Anatolian Fault [*Dor et al.*, 2008], Arima-Akatsuki fault [*Mitchell et al.*, 2011]). It is characterized by an intense microfracturing, with many intragranular fractures, but with little strain recorded, as the initial microstructures are not disturbed. In the field, the rock may look fresh but is easily crumbled by hand. This microfracturing is extensive: zones of pulverized rock extending over several hundred of meters have been reported [*Dor et al.*, 2006; *Mitchell et al.*, 2011].

Pulverized rocks are surprising because strain has not been localized, as is commonly seen in nature and in laboratory experiments [*Hild et al.*, 2003]. During our research, we hypothesized that high strain rate loading would have inhibited strain localization. Pulverized rocks could therefore be records of previous large earthquakes occurring near the fault.

To test this hypothesis, we conducted experiments at high strain rate. Several questions were to be answered:

1. Can we reproduce pulverization ?

2. What are the conditions to get pulverization ?

3.1.1 Can we reproduce pulverization ?

We recognize experimentally pulverization as the lack of localization of damage and the fragmentation of the tested sample into multiple small fragments. The first experiments we conducted with rocks sampled near the Lake Hughes area, a road outcrop near the San Andreas Fault where intense pulverization was reported [*Dor et al.*, 2006]. The experiments were performed in the Ecole Polytechnique at the Laboratoire de Mécanique des Solides in collaboration with Gérard Gary.

We used Split Hopkinson Pressure Bars (SHPB) to load the sample uniaxially at strain rates between $50/s$ and $500/s$. At such rate, elastic wave propagation has to be taken into account. For
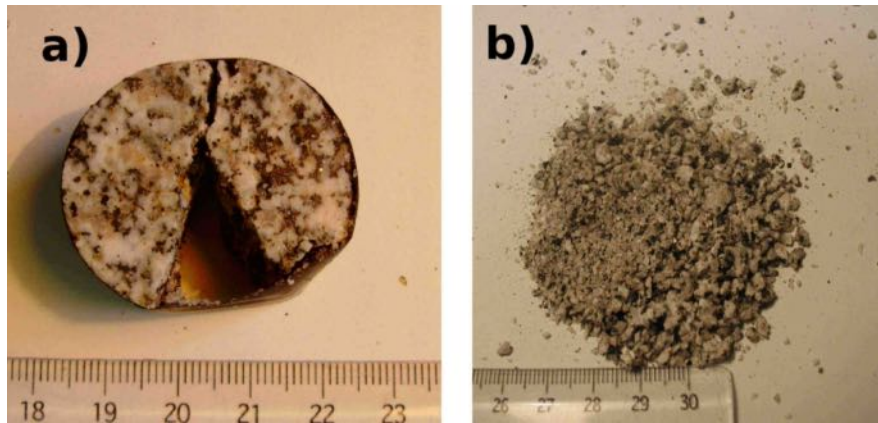
Figure 3.3: (a-left) At a low strain rate (here, 140/s), a granodiorite sample split into a few fragments when deformed in the Split Hopkinson Pressure Bar apparatus. (b-right) At a higher strain rate (here, 400/s), the sample was pulverized into numerous fragments with diameter smaller than the rock initial grain size. The ruler has centimetric marks. From *Doan and Gary* [2009]

instant, 1% strain at 500 /s is reached after 20 μs. During that time, stress waves propagate over 10 cm in a metal cylinder with P wave velocity of 5000 m/s. In usual rock mechanics rigs – and in the SHPB system – , stress gauges do not record the actual stress experienced by the sample. With the simple geometry of the SHPB apparatus, it is possible to retropropagate waves to the ends of the bars, hence to the edges of the sample. That is why SHPB apparatus are commonly used to perform high strain rate experiments [*Chen and Song*, 2010].

Yes, for crystalline rocks

The first set of experiments we performed was on natural granodioritic samples from the San Andreas Fault, near the Lake Hughes outcrop of pulverized rocks. We took non pulverized rocks sampled at about 100 m from the fault core, and used them as a proxy of the rocks before pulverization: damaged, but only slightly. The uniaxial high strain rate experiments provided only 3 outcomes [*Doan and Gary*, 2009]:

1. the sample was not damaged

2. the sample was split axially in a few fragments, no more than 5. This is the typical damage observed when a rock sample is uniaxially loaded at low strain rate [*Paterson and Wong*, 2005].

3. the sample was shattered in multiple small fragments, smaller than the initial grain size of about 1 mm. This diffuse damage is reminiscent of pulverized rocks.

We made other experiments on the Tarn granite, which we used as a proxy for undamaged rocks, and found again only these 3 states [*Doan and D'Hour*, 2012, Fig8]. Other authors working independently on Westerly granite found similar results [*Yuan et al.*, 2011].

No, for limestone

We also tried to reproduce pulverization on carbonate rocks [*Doan and Billi*, 2011], motivated by the observation of both pulverized granitic rocks and intact limestone on the same outcrop near Lake Hughes.

Contrary to the crystalline rocks, we think we did not achieve pulverization. First, in conditions where we collected multiple fragments, the final grains do not have a round shape, but a elongated needle-like shape not seen for crystalline rocks. Second, post-mortem samples that were jacketed and whose fracture pattern could be examined display a hierarchy of fractures (figure 3.4), suggesting
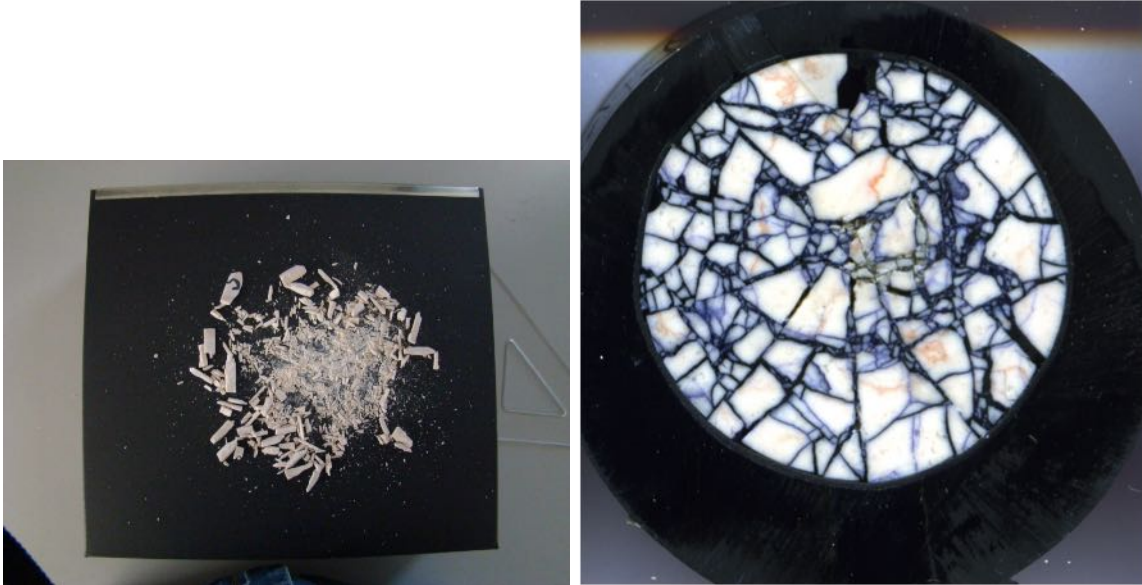
Figure 3.4: Cross-section from a "pulverized" marble sample (Sample B). Diameter is about 2.5 cm. There is a hierarchical fracture pattern, suggesting that deformation localized and the dense microfractured structure results from cumulated faults. On the unjacketed samples, the fragments have a needle shape pattern, suggesting that deformation occurs by accumulating tensile fractures perpendicular to the loading direction.

that tensile transverse deformation localized on a few fractures and create new blocks, and afterwards other fractures appear within each block. With increasing strain, intense microfracturing is observed, but with a different process from pulverized rocks: the multiple fractures appeared successively, but not simultaneously.

3.1.2   What are the conditions for pulverizing rocks ?

Strain rate effects on macroscopic damage

The intense fragmentation tends to happen at high strain rate loading. Figure 3.5 summarizes all the tests made on the San Andreas Fault samples [*Doan and Gary*, 2009]. Pulverization is achieved when strain rate exceeds a given threshold, here about 150 /s. This result is confirmed by other studies. For instance, we conducted a similar series of experiments on Tarn granite [*Doan and D'Hour*, 2012, Fig8], a non pre-damaged rock, for which the scatter of data due to variability is reduced. Similarly, *Yuan et al.* [2011] found also a threshold in pulverization on Westerly granite samples. In these two studies done on intact granitic rocks, the threshold in strain rate is also about 250 /s.

Such strain rate is not expected for a standard sub-sonic rupture propagating at a speed below the S wave velocity of the medium. Several hypotheses can be proposed to explain such high strain rate: supershear rupture [*Doan and Gary*, 2009], bimaterial interface [*Shi and Ben-Zion*, 2006] or local heterogeneities that accumulated energy and suddenly fail [*Dunham et al.*, 2003]. In all cases, pulverized rocks may be records of high frequency shaking, and it may be useful for paleoseismology.

Why does high strain rate favor pulverization ?

Several processes occur during damage of a rock: (1) crack nucleation where the local intensity factor exceeds a threshold, (2) crack coalescence and (3) crack propagation.

The classical model to describe rock failure at low strain rate is the Weibull model [*Weibull*, 1939]. It assumes that once a crack nucleates, it will propagate instantaneously and localize deformation. This model is valid if loading rate is so small that fracture propagation can be neglected. Given a statistics of fracture length, a statistics of failure probability with applied stress can be determined.
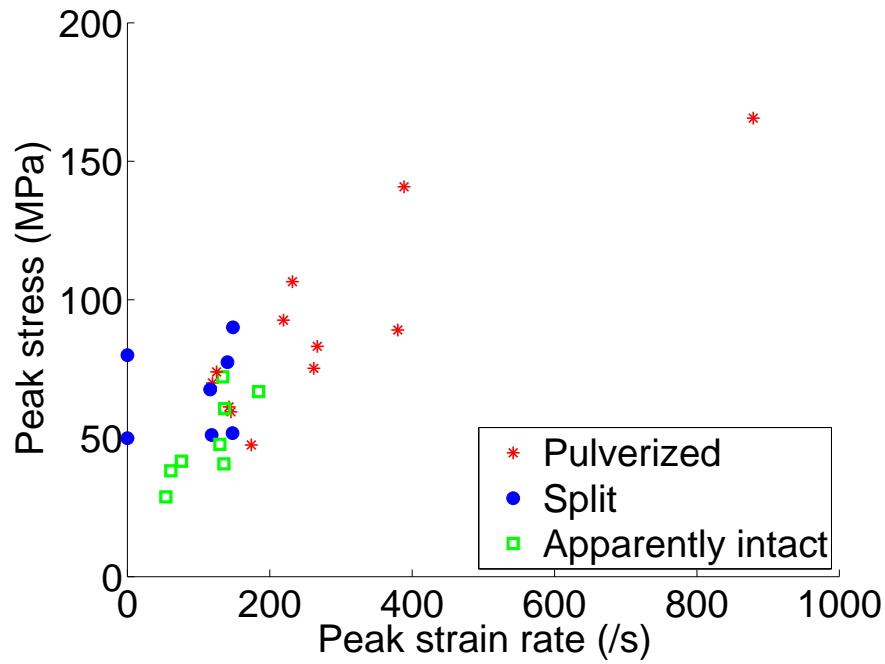
Figure 3.5: Summary of the high strain rate experiments conducted on the samples from the San Andreas Fault. We report the final state of the sample, as a function of the maximum stress reach and the maximum strain rate experienced during the loading.
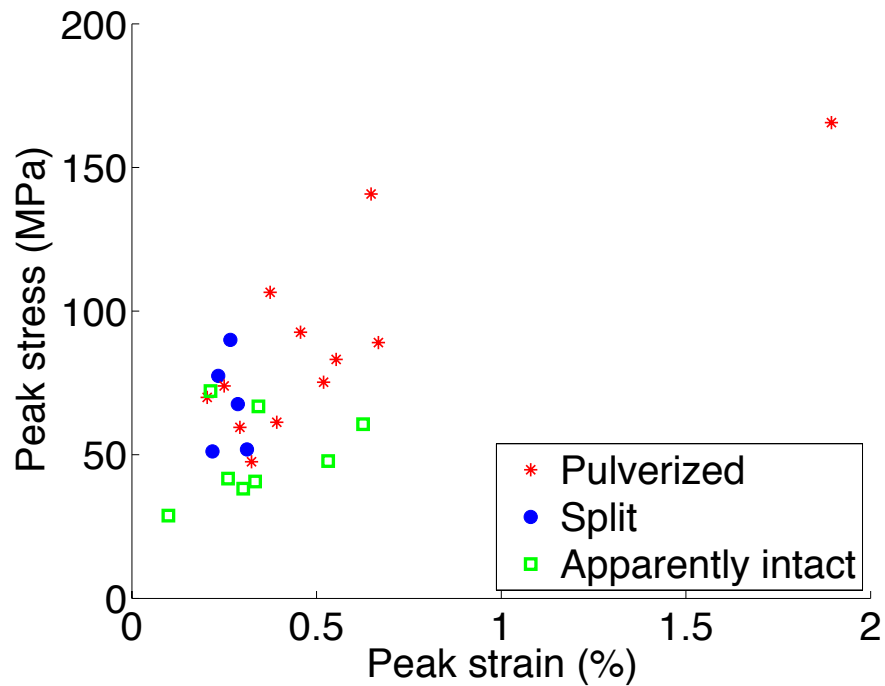

Figure 3.6: Summary of the strain reached for the same experiments as in figure 3.5.

The model of *Denoual and Hild* [2000] explains how multifracturing occurs at high strain rate. The favorable fractures prevent the nucleation of other fractures. This changes the density of fracture that can be activated. They couple the density of fractures with a mean-field theory, where local stress is screened by a damage parameter directly dependent of the density of fracture. They find that strength increases beyond a threshold stress rate, similar to the threshold we detected.

We use this model to interpret the threshold of strain rate and the influence of initial damage on our results [*Doan and D'Hour*, 2012]. The threshold diminishes with the increasing initial density of flaws. A rock next to a fault experiences many earthquakes, and are loaded repeatedly. One can expect that once a rock became pulverized, its flaw density increases sharply, so that it pulverizes more easily during the next loading, leading to the occurrence of extremely comminuted rocks. On the other hand, rocks with high pulverization threshold would not enter this feedback process. Competent rocks and pulverized rocks could therefore next to each other on the same size of the fault, as observed on the Lake Hughes outcrop on the San Andreas Fault [*Dor et al.*, 2006].

Discussion: what are the influence of parameters other than strain rate on our results

We discussed so far the trend to get pulverization at high strain rate. However, several parameters affect the macroscopic failure state.

The first one is the strain experienced by the sample. We expect a correlation between high fracture density and strain: even if microfracture propagation is not localized, damage accumulates with strain as seen in section 3.1.1. Moreover, Split Hopkinson Bars cannot be servocontrolled: if the damaged sample fails, it may accumulate large damage as the loading is not stopped at the onset of failure. To limit strain, we use a shorter striker to limit the loading duration. In the data set of *Doan and Gary* [2009] (figure 3.6) pulverization is not always systematically associated high strain, at it occurs sometimes with the same strain as for axially split sample.

There are also artifacts related to the structure of the sample. The major one is the effect of dynamic confinement, that results to the slow lateral expansion of the sample (controlled by stress wave propagation) compared to its loading rate. With lateral confinement above $\sim 15\,MPa$, failure mode of Westerly Granite switched from axial splitting to shear fracture [*Waversik and Brace*, 1971]. When estimating lateral confinement with the formulation of *Forrestal et al.* [2007] for our test, a maximum value of $\sim 10\,MPa$ was reached, with most values around $2\,MPa$.

In conclusion: strain rate is a key parameter to pulverizing rocks. However, other parameters may not negligible and should be systematically checked in later studies.

3.2 Microscopic characterization of dynamic damage

Macroscopic description of damage is a convenient way to assess damage patterns, but its lacks quantitative description. To get descriptible states of damage, the samples were jacketed by a shrinkable jacket. In the study of *Doan and Billi* [2011, Fig3], this jacket did not alter the mechanical data. We made with Andrea Billi a preliminary observation of microstructure on limestone. With Tom Mitchell we improve further the microstructural and petrophysical studies of the samples.

Note that in this section, we do not focus on pulverized rocks only, but on any structures that could be associated with dynamic damage.

3.2.1 Reproduction of microscopic pulverization

One of the initial projects we conducted with Tom Mitchell was to investigate the effect of multiple high strain rate loadings on the microstructure. We took care to apply small strains to better preserve microstructure. To our surprise, the apparently intact samples display intense microscopic damage (figure 3.7,[*Mitchell et al.*, 2013]). No macroscopic fractures appeared, as the microfractures did not coalesce. Although we were below the strain rate threshold characterized macroscopically, damage was diffuse within the sample, as for pulverized rocks.

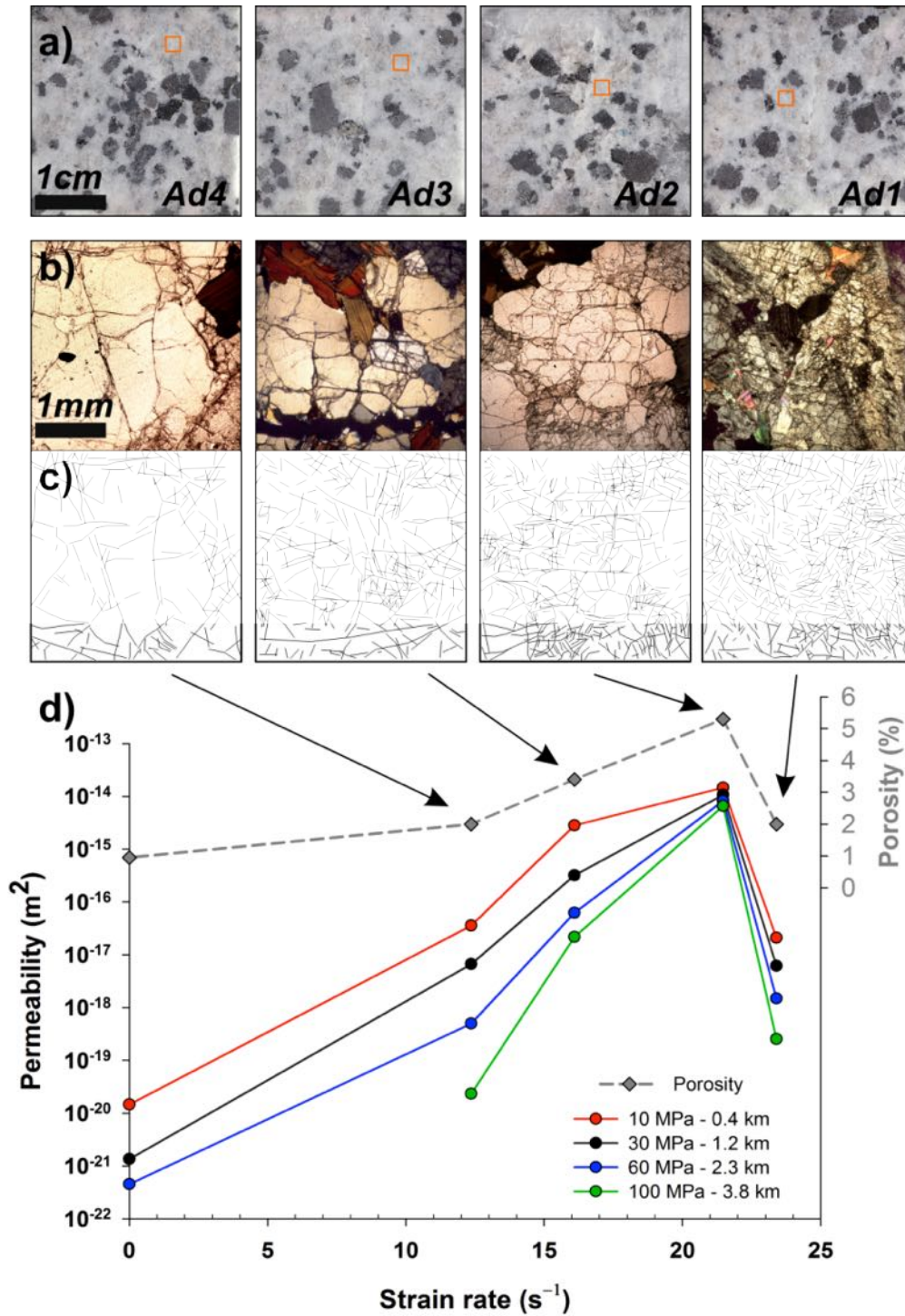Figure 3.7: Microstructures obtained from high strain rate experiments. (Top) No fractures are visible at the macroscopic scale. (Middle) Thin section observation of the same samples as in top figure shows intense microfracturing. (Bottom) Permeability measurements shows permeability enhancement by more than 5 orders of magnitude, in a pattern similar to natural observations on the San Jacinto Fault. After *Mitchell et al.* [2013]
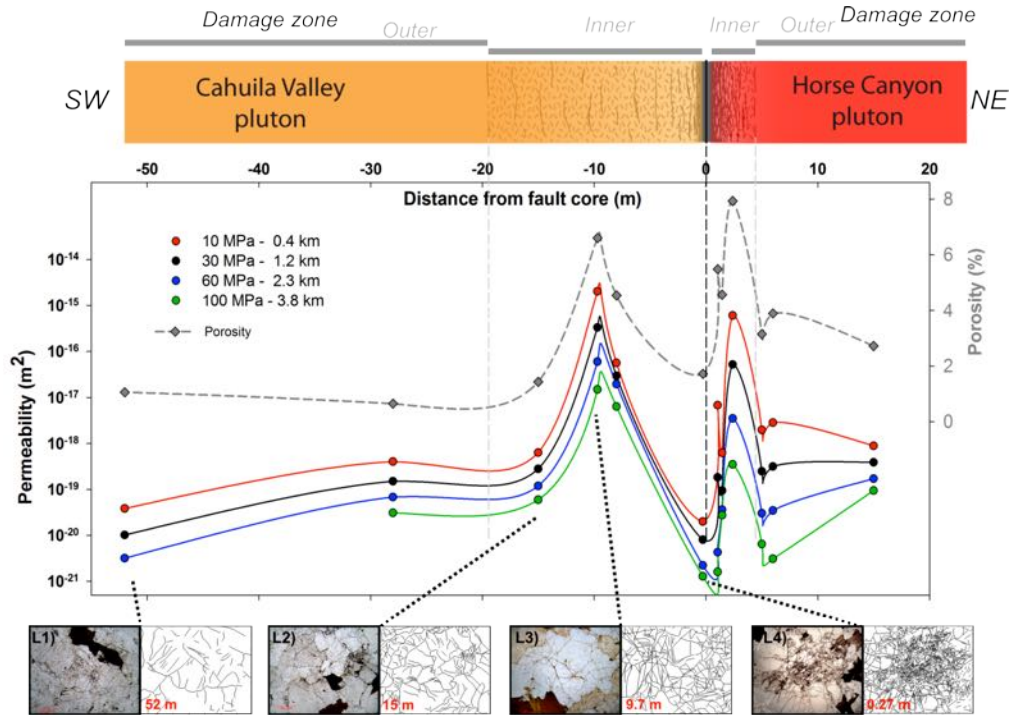
Figure 3.8: Permeability profiles measured on cores collected across the San Jacinto Fault. Permeability values and microstructures are similar to the experimental ones (figure 3.7). After *Mitchell et al.* [2013].

3.2.2 What are the transport properties of rocks damaged dynamically?

As my field work mainly focuses on the hydrological properties of faults, I will discuss here the major results retrieved on permeability and healing properties of rocks damaged at high strain rate.

Permeability

With Tom Mitchell, we were interested to the permeability of the samples damaged at high strain rate. We damaged together tonalite samples at low strain and moderate strain rate (figure 3.7). The samples were thereafter inserted it in a permeability measurement cell and confined with effective pressure up to 90 MPa. Some samples exhibit a permeability enhancement by 5 orders of magnitude, associated with the intense microfracture pattern, similarly to natural samples (figure 3.8). Note that in both natural and experimental results, the maximum permeability is not reached for the most fractured rocks. A possible explanation is that fracture lengths are smaller in pulverized rocks. As fracture width increases with fracture length, and permeability scales as the cube of fracture width, permeability is reduced despite the higher fracture density.

This dynamic enhancement of permeability has potential application on the mechanics of the seismic rupture. The early shaking due to seismic waves propagated ahead of a dynamic rupture can increase permeability and decrease the potential for thermal pressurization. It alters fluid transport, that could be of importance for subsequent healing processes.

Change in healing processes

Fault heal through many processes. One of the major process is pressure-solution, which is more efficient with smaller transport distance [*Gratier and Gueydan*, 2007]. For pulverized rocks, this distance is controlled by inter-fracture distance and is hence very small, which fosters intense pressure-solution. During the PhD of Julie Richard (co-supervised with Jean-Pierre Gratier), we conducted healing experiments on porous limestone (Estaillade Limestone) by percolating reactive fluids through the samples during several months. We encountered many experimental issues and the results are currently being analyzed. Yet preliminary study show promising results, with a very different behavior
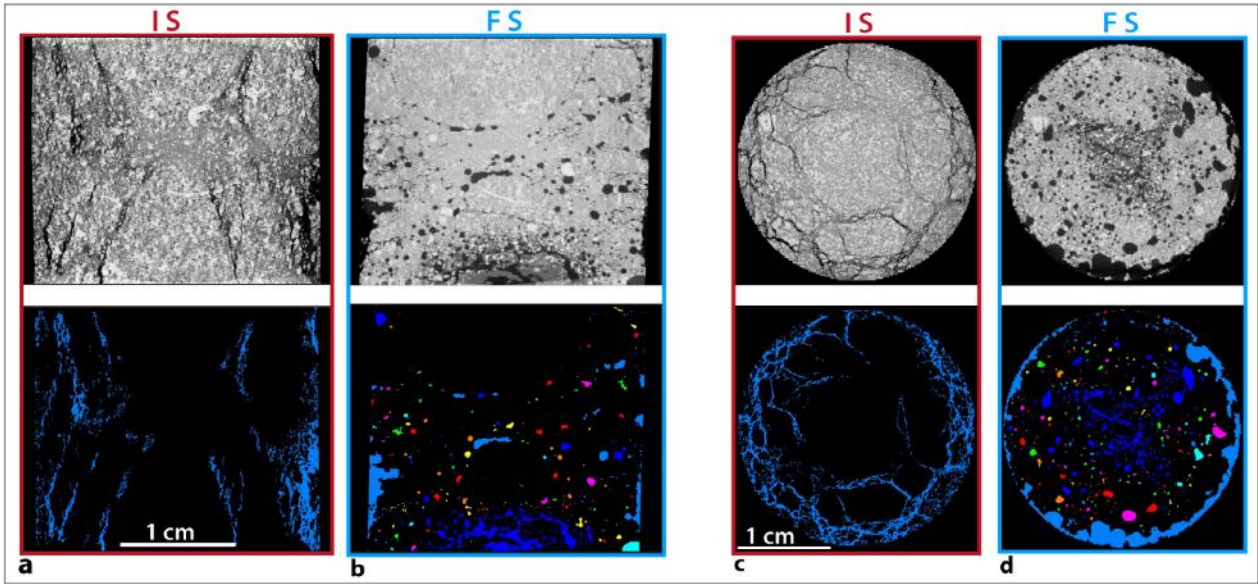
Figure 3.9: Postmortem structure after percolation of reactive fluids from X-ray CT Scan imaging. Left part gives vertical section of the initial state (IS) and final state (FS) of the sample. Right part shows cross sections of the bottom of the same sample. From *Richard et al.* [2014b]

.

for an intact sample and microfractured sample, as seen from X-ray CT scan images. For the microfractured sample, large dissolution features like round cavities coexist with zone apparently sealed. The occurrence of such features are very limited for the intact sample. In the case of active faults, damage associated to earthquakes is expected to greatly activate the geochemical processes: transport of fluids from depth, healing and creeping by pressure solution [*Gratier*, 2011].

This study is to be extended during the PhD of Frans Aben (in co-supervision with François Renard), we plan to foster with study, especially to monitor permeability evolution with time.

3.3 Conclusions

High strain rate damage seems to have a specific signature, with the extension of several fractures simultaneously. This creates a dense network of smaller fractures that changes dramatically the properties of the faults during the various phases of the coseismic cycle. The large increase in permeability can inhibit thermal pressurization during the coseismic cycle. The denser network of faults is associated with permeability changes, which may be economically interesting. It also enhance creeping processes like pressure solution, that is also involved in fault healing. As pulverized rocks are substantially weaker [*Rempe et al.*, 2013], it can reduce the apparent friction properties at regional scale [*Faulkner et al.*, 2006].

For instance, on the Northern Anatolian Fault, a fault segment entered a long-term creeping phase after a supershear earthquake [*Çakir et al.*, 2012]. Dynamic damage is a possible cause of this switch in frictional behavior. One can infer that the supershear rupture created diffuse damage near the fault. The weakening of rocks decreases the strength of the core and its surrounding damage zone. Meanwhile, pressure solution activates creep. To check such a hypothesis, in situ observation are needed. Within the framework of the Flow Trans Project, a Marie Curie Initial Training Network focus on Flow in Transforming media, a team from Grenoble plans to combine outcrop studies, InSAR monitoring and laboratory experiments to understand the dynamics of the Northern Anatolian Fault. This project funds the PhD of Frans Aben (starting October 2013), that I co-supervise.

Chapter 4

In-situ measurements of hydraulic properties across active faults

Estimating permeability along faults is key to understand several stages of the seismic process. For instance, large permeability following earthquakes explains the occurrence of ore deposits of economic significance along faults [*Sibson*, 1992]. Permeable fault about to rupture may experience anomalous precursory activity before an earthquake, like radon emission [*Ioannides*, 2003] or methane emission accompanied by bubbling [*Tary et al.*, 2012]. Clay-rich gouge of low permeability are amenable to pressure solution [*Wibberley and Shimamoto*, 2005].

However, determining permeability is difficult. Outcrops of former active faults were exposed through erosion and therefore experienced decompression and erosion. Permeability was not preserved. Boreholes give direct access to fresh outcrops, but cores were also decompressed. In situ measurement gives the best insight of hydraulic properties within faults. It enables to explore the scale dependence of permeability [*Boutt et al.*, 2012].

Two kinds of measurements are possible:

– Direct permeability measurement, through pumping tests. The scale of the rock mass investigated depends on the duration and the flow rate of the pumping test. I performed such tests were performed with the Modular formation Dynamics Tester (MDT) tool, as part of IODP expedition 319.

– Indirect permeability measurement through geophysical logs. We use datasets of IODP 319 to derive continuous permeability profiles and compare them with direct permeability measurements made with the MDT. The technique can also be used a posteriori on datasets from SAFOD.

During the last 15 years, several drilling projects gave new insight on fault mechanics at depth. Table 4.1 summarizes the major projects. Many projects (Nojima, TCDP, WCDP, J-Fast,...) were motivated by a devastating earthquake, and enable to study the distribution of fault slip across the fault zone, get insight of the rupture mechanism and monitor the postseismic healing of the fault. Others, like SAFOD, CRL, DFDP or GONAF aim at characterizing a major fault expected to break soon .

I had the opportunity to be involved in many of these drilling projects.

Project	Year	Fault depth (m)	Objectives	Hydraulic properties
Nojima Kobe earthquake, Japan	1995	300, 700, 1100	Post-earthquake characterization	Cross-hole testing
Corinth Rift Laboratory Greece	2004	750	Fault characterization and monitoring	Long term pore pressure monitoring
TCDP Chichi earthquake, Taiwan	2004	1111, 1138	Post-earthquake characterization	Cross-hole testing
SAFOD San Andreas Fault, CA	2004-2007	~ 2700	Fault characterization and monitoring	
NantroSEIZE Offshore Japan	2004 2009	~ 2700	Fault characterization Fault monitoring	MDT Pumping test Long term pore pressure monitoring
J-FAST Tohoku Earthquake, Japan	2011	750	Post-earthquake characterization	Long term monitoring
WCDP Wenchuan Earthquake, China	2009	~ 2700	Post-earthquake characterization	Long term monitoring
DFDP Alpine Fault, New Zealand	2011 2014	100, 150 ~ 1400	Fault characterization Pre-earthquake characterization and monitoring	Pumping test Long term monitoring
GONAF Northern Anatolian Fault	??	??	Pre-earthquake characterization and monitoring	Long term monitoring

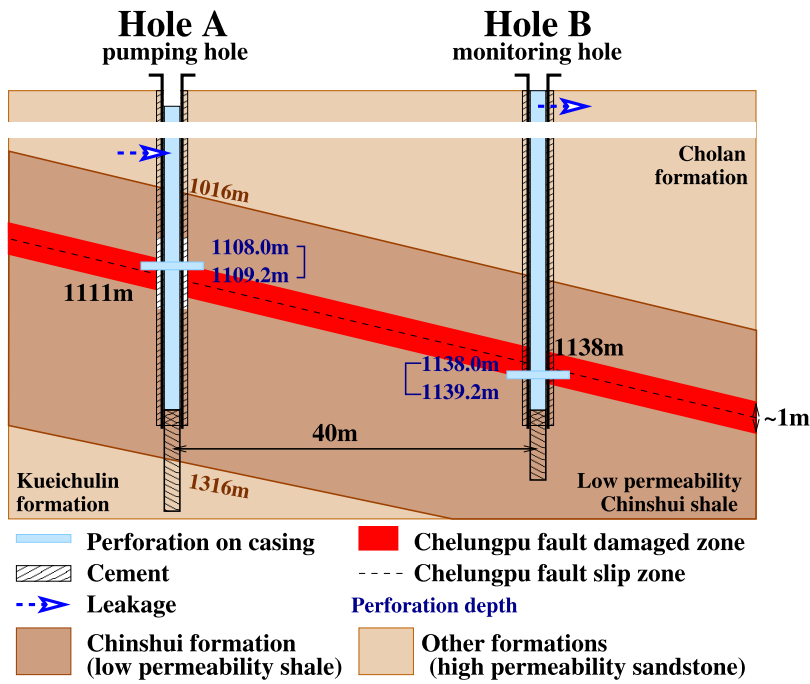Table 4.1: Table of the major projects drilling an active fault.

Figure 4.1: Cross-hole experiments at TCDP borehole enabling to determine the permeability of the damage zone of the Chelungpu Fault. From *Doan et al.* [2006a].
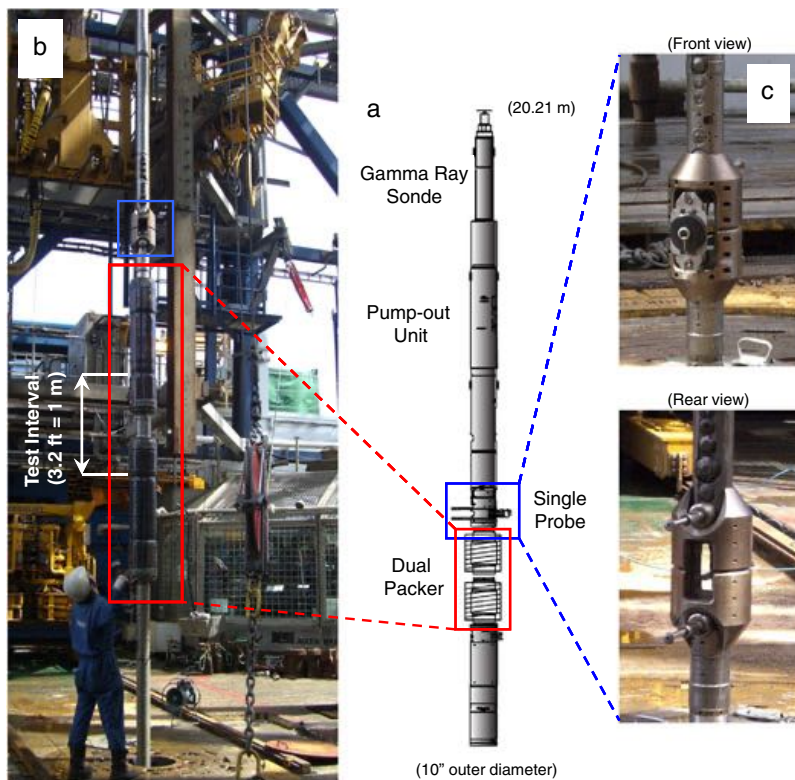

Figure 4.2: Modular formation Dynamics Tester (MDT) enabling to perform hydraulic tests and hydrofracturing at depth. From *Ito et al.* [2013].

4.1 Direct pumping tests

Pumping tests provide information on all hydrological parameters: current pore pressure, permeability and hydraulic diffusivity (and hence storativity). The volume scales as a power 3/2 of the duration of pumping, enabling to investigate the hydrological properties at large scale.

4.1.1 Cross-hole testing along Chelungpu Fault, Taiwan

As part of my postdoctoral studies, I could perform a slug test through the damage zone of the Chelungpu Fault, at the origin of the Chichi earthquake in 1999 [*Doan et al.*, 2006a]. On its northern strand, the fault experienced little acceleration but large displacement during the earthquake, and thermal pressurization was suspected to have weakened the fault. This mechanism needs low hydraulic diffusivity to maintain the high pore pressure generated by the seismic slip. We had the opportunity to use two holes drilling by the Taiwan Chelungpu-fault Drilling Project (TCDP). They were cased and perforated at the location the damage zones above and below the fault core (figure 4.1). We performed cross-hole pumping test, avoiding the influence of drilling-induced perturbation around the drillholes. As what happened during the pumping tests performed on Nojima Fault, the tests were disturbed by leaks induced by poor well completion. In our cases, we could correct our data by measuring and characterizing the leaks prior to the test. We could retrieve reliable values of hydraulic diffusivity of $(7 \pm 1) \times 10^{-5} \, \mathrm{m^2/s}$. This value is low enough to suggest that thermal pressurization is a viable weakening mechanism [*Doan et al.*, 2006a].

4.1.2 Exploiting the MDT tool data provided by the NanTroSEIZE project

I had another opportunity to perform hydraulic tests in situ within the framework of the project NanTroSEIZE (Nankai Trough SEIsmic Zone Experiment). This project aims at understanding the Nankai Trough, performing a transect with boreholes along various location of the subduction zone [*Tobin and Kinoshita*, 2006]. I was part of IODP expedition 319, a technological mission, where the first riser drilling in IODP history were performed in hole C0009 [*Moe et al.*, 2012]. The Kumano Basin was of little interest for the knowledge of the seismic conditions of the Nankai Trough, but it provides a simple and safe environment for scientists with experience in continental drilling to test the new methods made possible by the better drillhole and the larger pipe diameter. Among the available tool was the Modular formation Dynamics Tester (MDT) by Schlumberger. This tool embeds two pumping tests apparatuses (figure 4.2):

1. A single probe pushing a packed against the borehole wall and pump water out of a small chamber of 5 cc. This small volume enables a rapid recovery from the pumping. It provides a rough estimate of permeability (but very dependent on borehole conditions) and very importantly provides information on the local pore pressure conditions. From this tool, we could interpolate a pore pressure profile with depth, here very close to the expected hydrostatic value [*Saffer et al.*, 2013].

2. A dual packer probe, that enable to test a borehole section about one meter long. On this section, either pumping test to determine permeability or hydrofracturing is possible. In the former case, we retrieve a reliable value for permeability that is significantly higher than the permeabilities retrieved from core [*Boutt et al.*, 2012]. In the latter case, we retrieve information on the local stress field (at least, the minimum principal stress value perpendicular to the borehole direction) [*Ito et al.*, 2013].

Direct tests made in borehole provide reliable measurements, at the relevant scale and in quasi-pristine in-situ conditions. However, they provide very local information and questions arise on their spatial relevance. For instance, is there a lot of heterogeneity along the borehole?

4.2 Assessing hydraulic profiles from logs

Geophysical logs are quasi-systematically done after drilling, as they document the borehole conditions. They provide a continuous set of physical data: resistivity, seismic velocity, natural radioactivity, attenuation of gamma-rays and neutron, ... These logs may be of lower profile than the MDT tool and they tended to be left aside by most of the scientific party of IODP expedition 319, yet with them I could extract several information of interest:

1. Using the caliper data associated with the FMI, an electrical imaging tool, I could show that the borehole section below the Kumano Basin was deformed in a N135° direction. This direction is consistent with the almost invisible breakouts and the poorly clear drilling-induced tensile fractures. It shows that the maximum horizontal principal stress direction is parallel to the convergence vector between Japan and the Philippine Plate [*Lin et al.*, 2010].

2. The sonic data are sensitive to porosity. By calibrating semi-empirical laws with core data, I was able to retrieve a full profile of macroscopic porosity along the borehole [*Doan et al.*, 2011]. Comparing with the total porosity profile, this method quantifies the water absorbed in swelling clays, like smectite. It could be used in a latter stage of the NanTroSEIZE project to track the smectite-illite transition.

3. The electrical data are disturbed by the invasion of the vicinity of the borehole by drilling fluids. The separation between the shallow resistivity curve and the deep resistivity curve hints how permeable is the drilled medium. In case of hole C0009, invasion is extensive, suggesting a
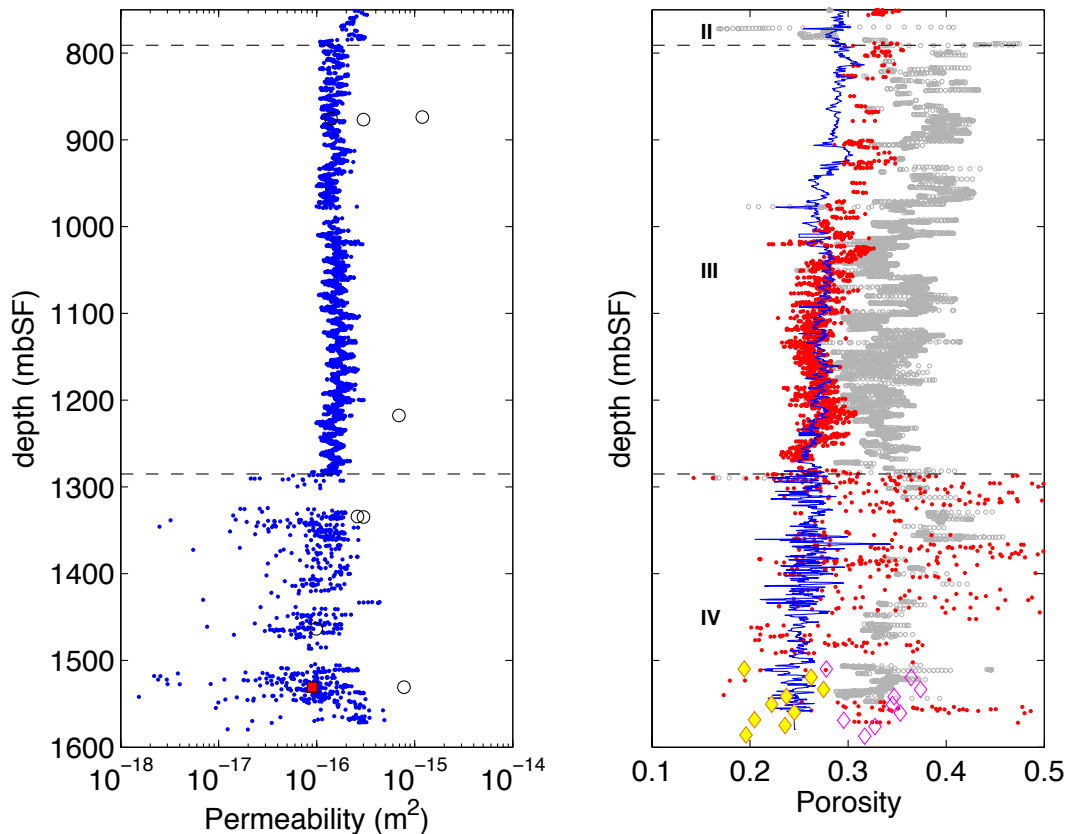
Figure 4.3: Geophysical logs enable to extrapolate the pointwise data acquired from cores and MDT data. (Left) We could retrieve a full profile of permeability from mud invasion recorded from laterolog resistivity data that compare well with MDT data, either single proble (open circles) or dual-packer (red square). (Right) We could get a continuous estimate of full profile of both macroporosity (red: resistivity data, blue: sonic data) and total porosity (grey: lithodensity).

mud cake of poor quality. We quantified the invasion process to retrieve a quantitative profile of permeability. We obtained a quantitative change in permeability when lithology changes: we could retrieve at least a good qualitative profile of permeability.

The quantification of invasion process with the electrical data is a promising tool to estimate the extent of the damage zone near an active fault. It is expected to be larger in the more permeable formation. We tested this hypothesis on two boreholes intersecting an active fault.

The J-Fast drilling is an offshore drilling project at the toe of the subduction fault that ruptured during the Tohoku earthquake in March 2011. Two boreholes were drilled, one with Logging While Drilling (LWD), the other without any logging. The LWD data were acquired a few minute after the drilling, and invasion is too limited to be perceptible.

We has better success, with the SAFOD project. Thanks to its free data policy. I could download the logging data. The shallow and deep resistivity of the laterolog data recorded a few days after drilling documents a zone with higher invasion (and no caliper anomaly) in the arkosic sandstone west to the fault. The damage is asymmetric and far from the fault. This zone is also consistent with a zone of large H_2 emission, that has been attributed as mechano-chemical hydrogen by *Wiersberg and Erzinger* [2008]. It would not be surprising that this zone has larger permeability, so that it canalizes radon emission [*Wiersberg and Erzinger*, 2008]. This zone may be the location of intense micro-mechanical damage, similar to the pulverized rocks, but at depth.

On the other hand, the so-called 200 m thick "damage zone" in figure 1.1 is impermeable with little separation between the deep and shallow resistivity. Geochemistry also suggests that little radon or hydrogen is emitted from the fault core. San Andreas Fault may be an hydraulic channel, but mainly within a "permeable" zone in arkosic sandstone, decoupled from the mechanically weak San Andreas Fault, that is impermeable.

4.3   Long term monitoring of pore pressure

Pore pressure is a key factor on fault mechanics. High fluid pressure reduces the effective Coulomb stress and weakens the fault [*Rice*, 1992]. Many attempts were done to record continuously fluid pressure within faults, but they are rarely successful due to the difficult drilling conditions next to the fault. For instance, the observatory installed within the SAFOD main hole lasted only a few weeks due to intense corrosion. Successful monitoring examples in continental drilling are the Corinth Rift Laboratory (but data documents the aquifers next to the fault), WCDP (but data record rather the damage fault next to the footwall) and the New Zealand DFDP (but at that stage, holes are shallow).

Long term monitoring provide many invaluable information. It provides reliable fluid pressure values, when borehole disturbances are dissipated. The recovery stage, of long duration, also documents hydraulic properties at large spatial scale. It also provides a dynamic view of the fault evolution. Rather than long term evolution associated with the seismic cycle, pore pressure monitoring also showed how faults are sensitive to triggering like teleseismic triggering [*Manga and Brodsky*, 2006] or permeability change following distant earthquakes [*Manga et al.*, 2012].

Access to these data is difficult, but I could get access to the dataset collected by the permanent observatory installed during the stage 1 of the DFDP project.

4.3.1   Extracting hydromechanical properties from tidal analysis

Boreholes tapping confined reservoirs commonly exhibit periodic variations in pressure with two dominant periods: diurnal (~ 24 h) and semi-diurnal (~ 12 h)[*Agnew*, 2007]. These oscillations reach 10 kPa and are easily recordable. Onshore, Earth tides induce these pressure changes, whereas oceanic boreholes are dominated by oceanic loading [*Wang and Davis*, 1996; *Davis et al.*, 2000].

Earth tides have the immense advantage of being predictable. By comparing the actual observations and the predicted deformations, one can retrieve information about the formation surrounding
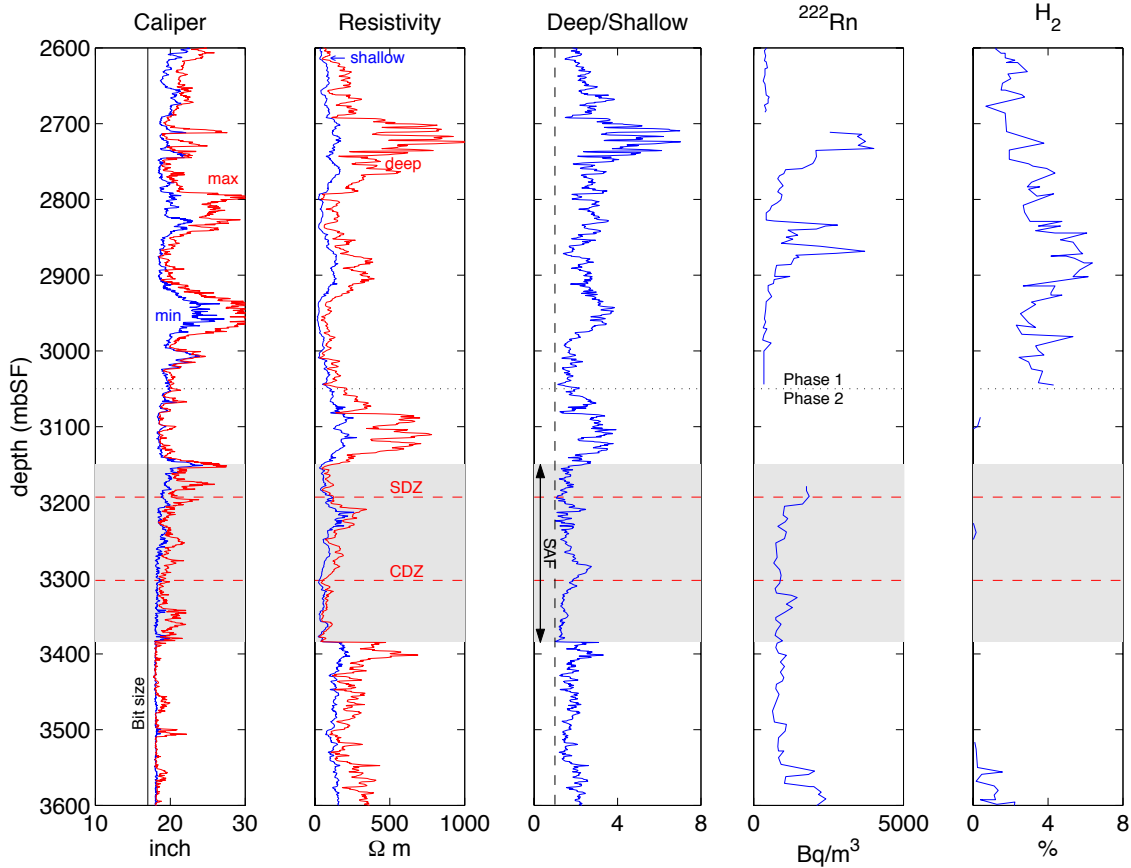
Figure 4.4: Resistivity logs showing differences in fluid invasion within the main hole of the SAFOD Project. The separation between the deep and shallow resistivities is not due only to change in borehole diameter, but rather to the permeability of theformation. The recognized creeping strands (Central Deforming Zone and Southern Deforming Zone) are impermeable, whereas the host rock at the boundary to the fault core are the most permeable. Real time gas monitoring data also show that fluid migration stands outside the fault core.

the well. This process occurs in two phases: (1) the poroelastic phase, in which the tidal strain induces change a pressure in the equilibrium and (2) the hydraulic phase in which the change in pressure in the medium induces a change in pressure in the well. This is expressed in figure 4.5.

We applied this method to the hydrological data acquired by the permanent observatory installed within the Deep Drilling Fault Project (DFDP) on the Alpine Fault, New Zealand (figure 4.6). This fault has several interesting features that motivate the drilling project: (1) according to paleoseismo-logic studies [Berryman et al., 2012], the fault is about to rupture with a large magnitude earthquake (2) the fault has a reverse component of about $1\,\mathrm{cm/yr}$, advecting heat and rocks exhibiting ductile deformation. The DFDP project aims at better characterizing the fault properties by coring and logging and to monitor its long-term activity.

In 2010, the first part of project (DFDP-1) was conducted: two shallows holes were drilled to better characterize the fault geometry and properties (figure 4.6). DFDP-1 proved to be a great success with cores of excellent quality, especially within the fault core [Sutherland et al., 2012].
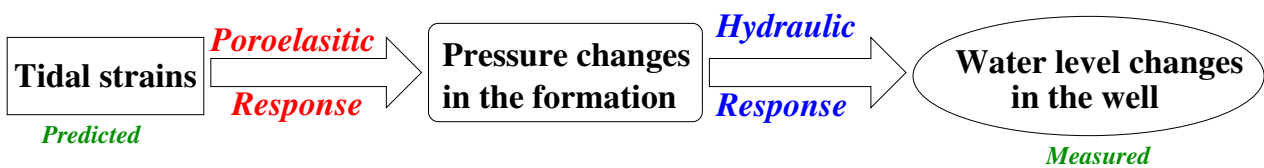
Figure 4.5: How the tidal strains are expressed as pressure changes. From Doan et al. [2006b]

Four piezometers were installed at four locations representative of zones of the fault structure: two were installed in the damaged hanging wall, one in the altered and cemented core and one in the footwall. In situ hydraulic tests performed just after drilling helped characterizing the permeability of the hanging wall with a high permeability larger than $10^{-14}\,\mathrm{m}^2$. Permeability measurement on cores gave a permeability of $10^{-18}-10^{-16}\,\mathrm{m}^2$ in the cataclasite, and $10^{-20}-10^{-19}\,\mathrm{m}^2$ for the gouge.
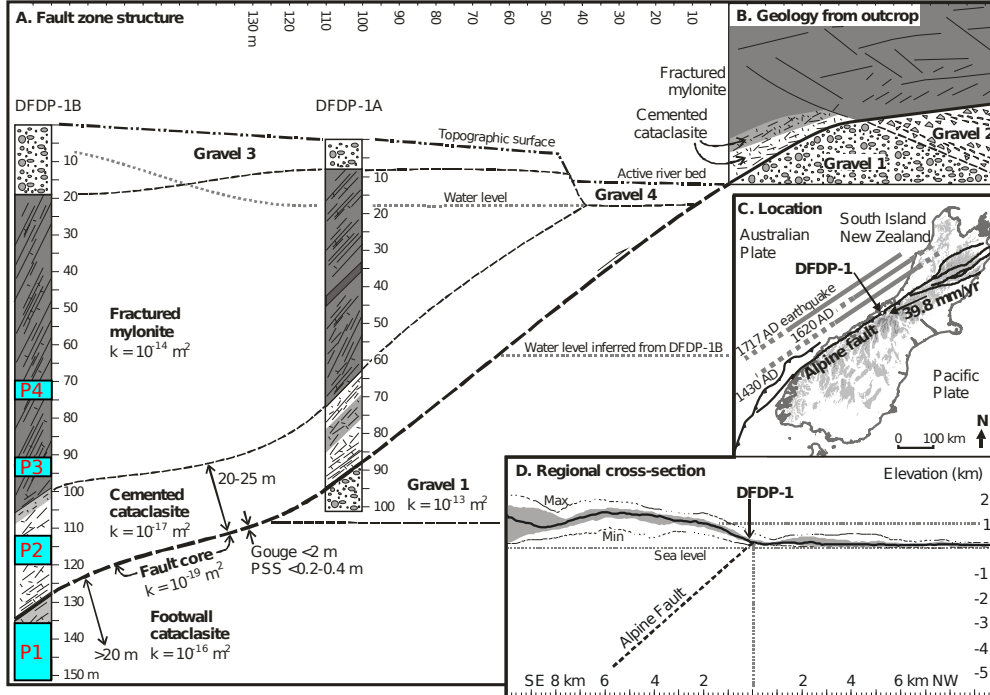
Figure 4.6: Summary of the results obtained by the first phase of the Deep Fault Drilling Project on the Alpine Fault, New Zealand, after *Sutherland et al.* [2012]. The DFDP1 project included the installation of an observatory within well DFDP1-B. We highlight with blue rectangles the intervals whose pore pressure was monitored.
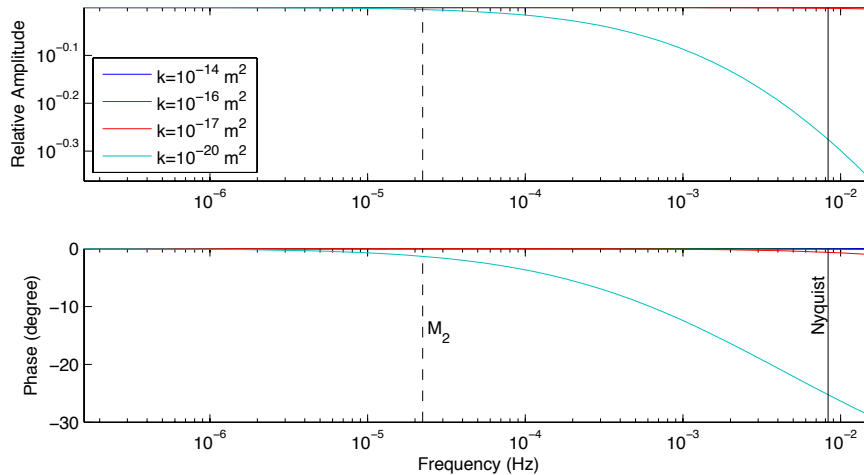
Figure 4.7: Theoretical gain response related to the hydraulic connection between the borehole and the formation. We used an adapted model [*Doan et al.*, 2006b] of the model of *Hsieh et al.* [1987] for closed wells.

With such values, it is expected that the pore pressure recorded in the borehole reflects the pore pressure evolution within the formation, without any phase lag (figure 4.7). Indeed, tidal fluctuations were recorded with high resolution. The amplitude of the signal is of high value, suggesting very tight formation (4.2). It confirms that damage zones around the fault are currently well cement. The

Data	Apparent BKu (GPa) (Mar11-Apr12)	Phase (Deg) (Mar11-Apr12)	Apparent BKu (GPa) (Jun12-Oct12)	Phase (Deg) (Jun12-Oct12)
P1	27.73	11.4	27.56	10.2
P2	28.4	13.9	28.7	13.3
P3	24.1	8.4	24.2	8.7
P4	16.4	10.3	16.7	10.4

Table 4.2: Tidal coefficient derived for M_2 tidal component derived from tidal analysis.

Figure 4.8: "Hydroseismograms" recorded by the DFDP1 sensors (figure /refDFDP1) during the arrival of the teleseismic waves emitted by the 2012 Sumatra earthquakes. During the passage of the first Rayleigh waves (R1), all pressure data are in phase. During the passage of the second Rayleigh waves (R2, after seismic waves travel around the Earth once), the signals exhibit different lags. Note that the x-axis are shown with the same scale. Y-data have been renormalized to highlight the similarity between each dataset.
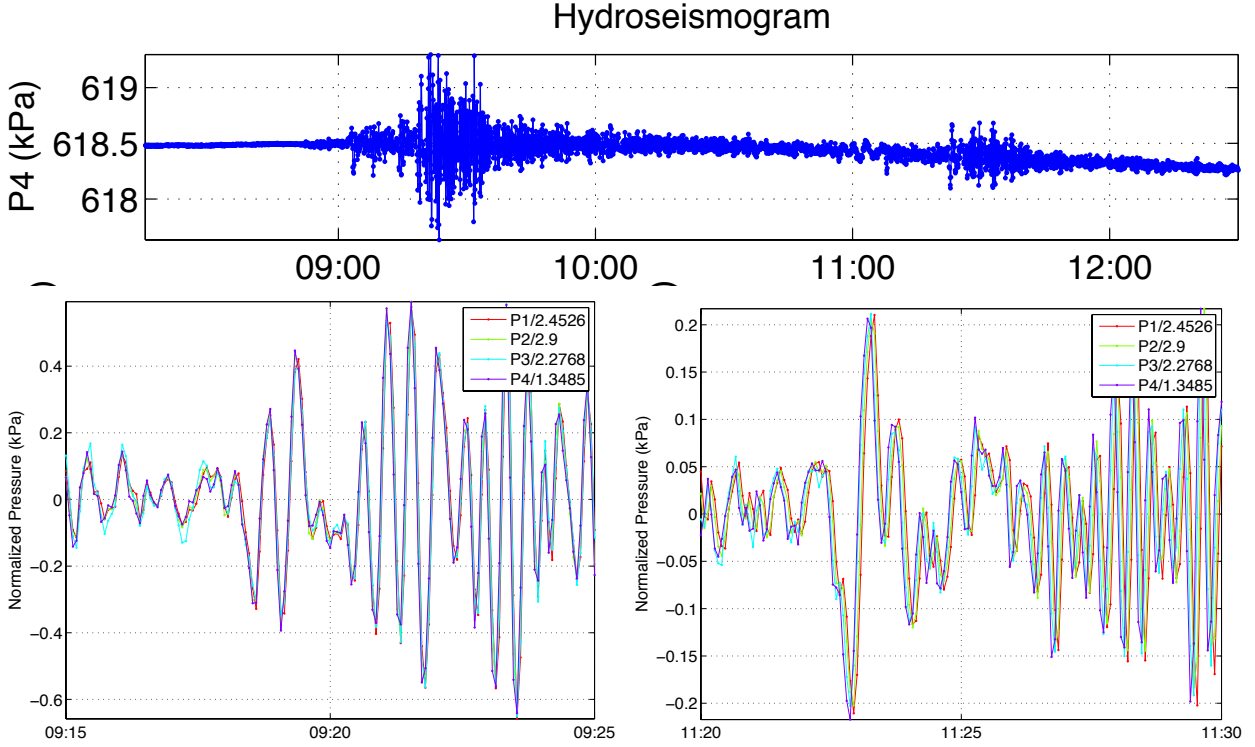
phase lag may be explained by anisotropy effect not taken into account the by Hsieh model *Hsieh et al.* [1987] In these conditions, we can record "hydroseismograms", where pore pressure reflects the strain induced by teleseismic waves. We had one example during in the DFDP monitoring, associated with the doublet earthquakes of Sumatra, April 2012. Figure 4.8 shows two time series of seismograms. During the first arrival of Rayleigh waves, all pressure data are in phase, consistently with theoretical predictions (figure 4.7). But during the second arrival of Rayleigh waves, both pressure sensors sampling the fractured zone of the hanging walls, get some phase shift. Both seismic signals have similar frequencies, and similar direction of arrival, so that anisotropic effects cannot explain the difference. The most probable reason for this delay is a change in permeability. The Alpine Fault is therefore sensitive to seismic waves. As it is suspected to be close of its critical state, it is important to continue to monitor how this sensitivity evolves with time.

4.3.2   Triggering of sliding episode of landslide within a clay-rich slope

Another example of long term monitoring of "fault" is the long term monitoring of the Avignonet landslide, a clay landslide near Grenoble. Previous geophysical investigation, including borehole drilling and surface geophysics proved that the landslide deformation is accomodated by several localized shear zones [*Bièvre et al.*, 2011] (see insert of figure 4.9). I proposed to monitor one of the shallowest shear zone with a high resolution sensor. The primary objective was to continuously monitor the hydromechanical evolution of the landslide from the tidal response. A first sensor was installed in 2010, recorded Earth Tides, but died out rapidly. A second sensor installed at the end of 2011 happened to be place in a more permeable formation and did not record tides. However, it enabled to record pore pressure evolution during more than one year, together with a lower resolution pressure sensor also located along the shear zone.

During winter, the clayish medium is saturated. However, during summer season, water level drawdowns, clays dry out and water level is not sensitive anymore to rainfall. The monitoring shows how the landslide becomes again sensitive to rainfall, and gets closer to critical state. First, the system becomes sensitive again to rainfall after a massive rain episode in October 2012 (step 1 in figure 4.9), but water level continues to decrease. Second, after another large rainfall episode, the water level stabilizes for all hydraulic sensors (step 2 in figure 4.9). The system gets closer to criticality: small amount of rain triggers a general disturbance of the landslide. Both hydraulic sensors experience a change in pressure (a decrease for the low resolution sensor, an increase for our high resolution sensor), as well as many other sensors installed along the landslide (Spontaneous Potential sensors, Time Domain Reflectometers).

4.4   Conclusions

Scientific drilling within active faults greatly improved our knowledge of the fault properties at depth, especially showing how slip get localized along thin principal shear zones of very low permeability for all drilling made in active faults. The in-situ characterization of hydraulic properties of faults was less successful. Few drillings completed the determination of a complete permeability log at the same scale and a successful installation of a monitoring system. A key issue is the poor well completion at the end of the drilling project, that impedes the pumping tests (TCDP) or prevent the installation of an observatory (SAFOD). Not surprisingly, one of the most successful project so far is the DFDP project, which has put hydraulic characterization of the fault to high priority. To get better results, fault hydrogeologists need to get involved earlier into the drilling projects.
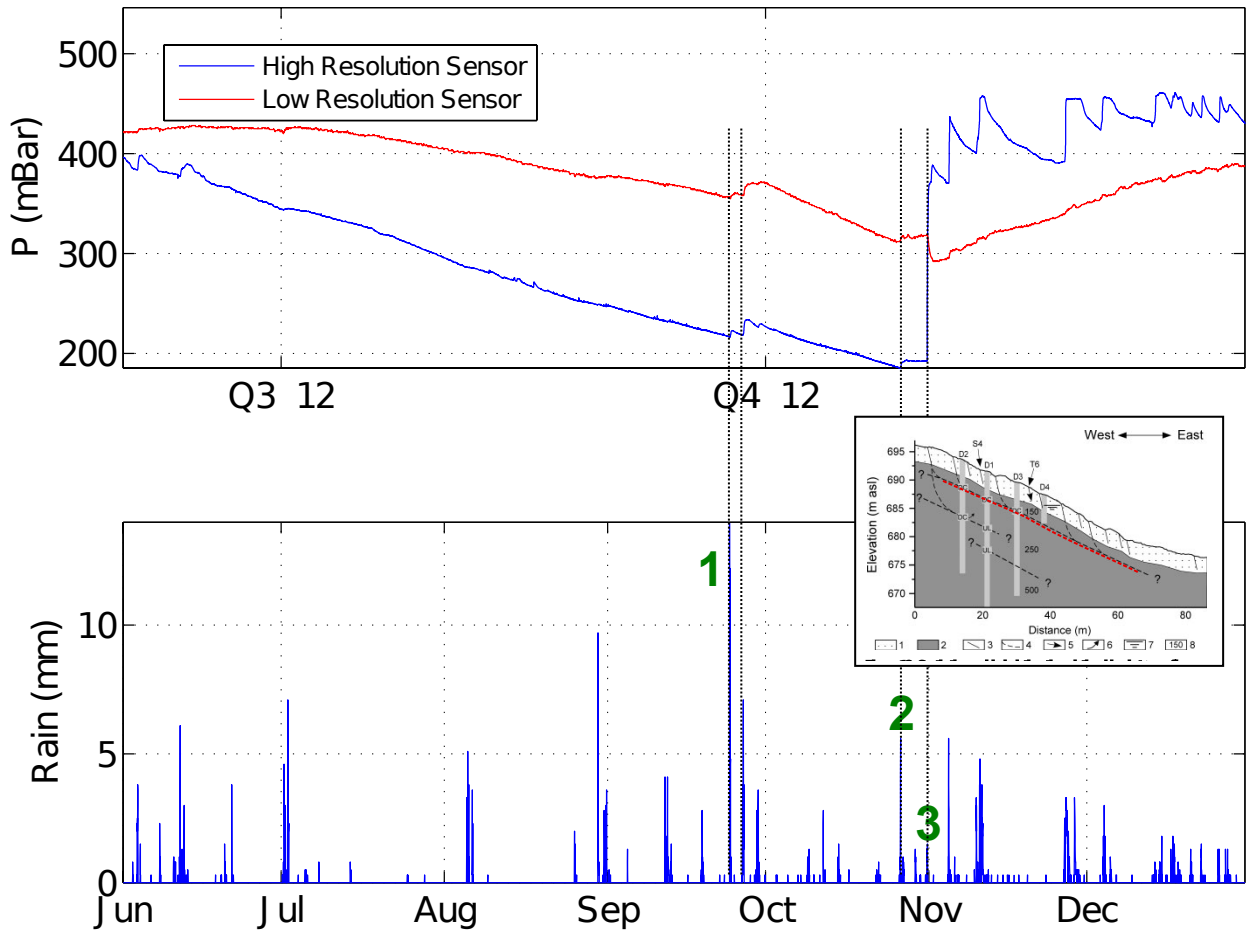
Figure 4.9: Hydraulic pressure recording within one of the main shear zone of the Avignonet landslide (red dashed line within the insert). The sensors record progressively greater sensitivity of water level fluctuations to rainfall. (1) After major rainfall, water level in the boreholes are once again sensitive to rainfall. (2) after another major rain episode, water level does not decrease any more (3) massive disturbance, with piezometric redistribution, occurs within the shear zone.

Chapter 5

Conclusions and Perspectives

5.1 Conclusions

In the previous chapters, I introduced the research I conducted on fault mechanics. Using borehole geophysics, I tried to characterize at from the metric to decametric scales a complete profilse of hydromechanical properties of active faults. This data is important since such scales are cumbersome to reach in laboratory experiment and tedious to quantify in outcrop studies. On the San Andreas Fault (section 4.2), the small separation between shallow and deep resistivities curves suggests that this mature large fault has developed more than 200 m of impermeable fault core, in which substrands localized still more deformation.The shallow DFDP holes drilled on the Alpine Fault, New Zealand, show more incipient alteration, which only began to make the fault core and its surrounding damage zone impermeable [*Sutherland et al.*, 2012]. These results differ from the Chelungpu fault, in which several fault zones were identified. The actual strand at stake for the 1999 Chichi earthquake was difficult to identify. Our hydrological study within its damage zone confirmed it was of high permeability for shale [*Doan et al.*, 2006a]. Alteration process is not as important for this fault.

The ability for a fault to reuse the same strand throughout its seismic cycle is therefore crucial for the evolution of the fault zone, of its healing and alteration processes. This issue is tackled indirectly by my experiments, either on the Split Hopkinson Pressure Bars or High Velocity Friction experiments: at high strain rate, finite wave propagation limits correlation lengths between heterogeneities and strain can get localized elsewhere than the favored heterogeneities (the largest fractures for pulverization, the gouge boundaries for friction experiments). Hence, jamming can occur in pure talc gouge leading to unexpected high friction [*Boutareaud et al.*, 2012]. Hence, multiple fractures can propagate simultaneously at high strain rate [*Doan and Gary*, 2009; *Doan and Billi*, 2011].

I think long term monitoring is the future of the understanding of active faults. On the example of Avignonet (section 4.3.2), in which the "fault" is a subsurface shear zone. We recorded what seismologists would have dreamed to record prior to large earthquakes: the progressive destabilization of the fault under an external factor (here, rainfall), progressively getting closer to criticality and finally being triggered by a small disturbance. At another scale, the observation of *Bouchon et al.* [2011] prior to the 1999 Izmit earthquake on the Northern Anatolian Fault suggests that slow slip may occur on active faults prior to major earthquakes. Such slow slip would be monitored by the observatories of the second stage of the DFDP project, of the NantroSEIZE project or of the "Geophysical Observatory at the North Anatolian Fault" (GONAF) project [*Dresen et al.*, 2008].

5.2 Future work

I developed two technical specialties that are relatively uncommon within the Earth Science community: (1) borehole hydrogeophysical studies of active faults (2) high strain rate damage mechanics. During the following years, I plan to continue to exert this dual approach to fault mechanics, by performing experiments in conditions closer to that of the nucleation zones of earthquakes.
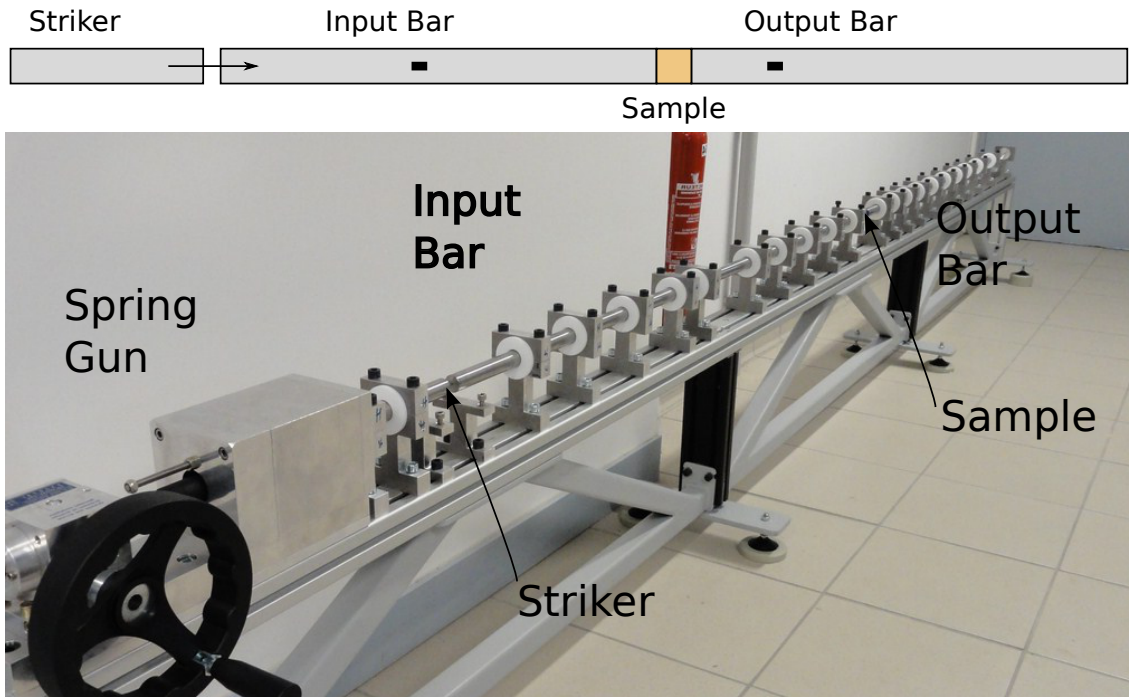
Figure 5.1: Mini-SHPB setup installed in Grenoble. This device enables to test small size samples (diameter less than 2 cm) at low strain but high strain rate. Its modular design make it easy to build up new instrumentation around the sample.

5.2.1 Experimental dynamic damage

My more immediate task on dynamic damage is to build my own experimental device. Indeed, it appeared that the remote location of the SHPB apparatus of École Polytechnique, next to Paris, combined with the retirement of Gérard Gary impeded to perform as many tests as needed. That is why we built our own system at ISTerre (figure 5.1). It is now ready, with a home-made interpretation program, and a reverse-engineered the amplification system. The mini-SHPB system has a modular design, to enable progressive enhancement with incremental funding. Another particularity of the design is its small size, with a maximum sample diameter of 2 cm. This size has several practical advantages: (1) the samples can be inserted in petrophysical apparatuses, such a permeameters, Brunauer–Emmett–Teller (BET) surfacemeters or the percolation cells of ISTerre, to get beyond simple macroscopic damage observation (2) the apparatus dimensions scale so that they just fit the experimental space available.

When we began to work on microscopic structures, we realized that diffuse damage can be generated by lower strain rate and lower strain than in our previous studies (section 3.2). We plan to couple more systematically the dynamic damage experiments with better characterization of damage patterns. In addition of thin sections, several petrophysical methods are planned to be implemented:

– P wave measurements are planned to be performed more systematically, with some plans to mount piezometers directly on the bars.
– Quantification of damage through BET measurement of surface area, that is expected to increase substantially for pulverized rocks. A study is performed in cooperation with Mike Heap to investigate the properties of volcanic rocks producing ashes.
– During the PhD of Frans Aben, starting October 2013, we plan to add permeability measurement capabilities to the percolation cells of ISTerre. They can be used to measure permeability of the damaged samples, before and during healing experiments.
– Spencer et al. [2012] have shown a reset of thermoluminescence data of SAFOD sample that may be remnant of the 1857 Fort Tejon earthquake. We plan to conduct dynamic experiments to control this hypothesis.
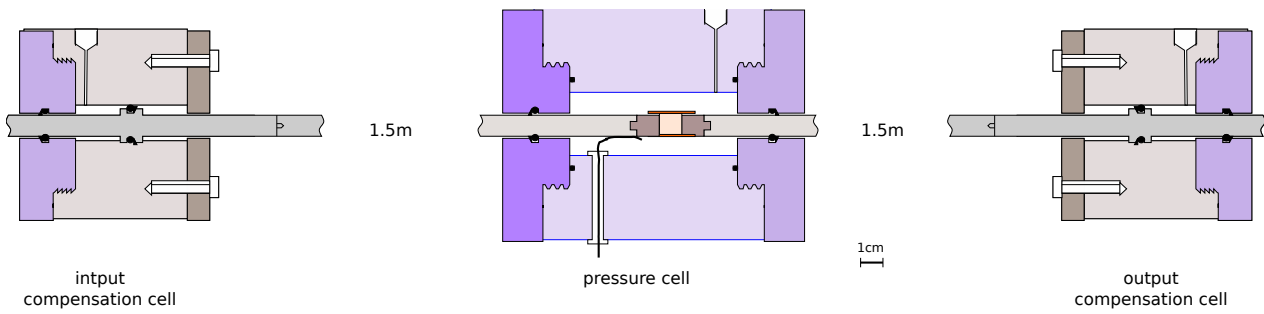
Figure 5.2: Dynamic confinement system that could be built of the mini-SHPB device (figure 5.1). The building of the experimental setup is ready but no funding was found yet.
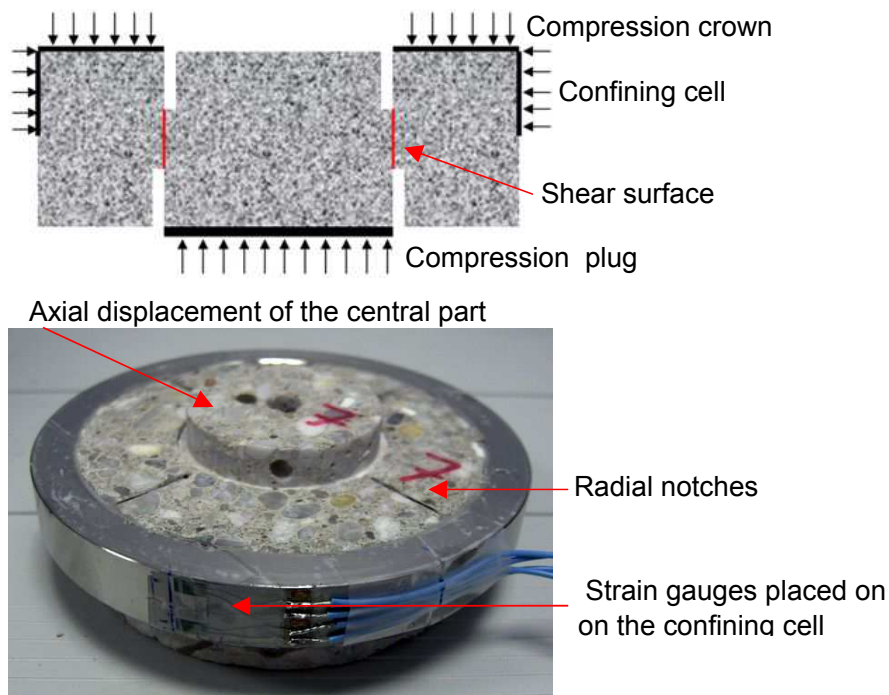
Figure 5.3: Punch-Through Shear test system used in a SHPB device by *Forquin* [2011]. We plan to test such a technique on the crystalline rocks tested in *Doan and D'Hour* [2012] to check the dependance of our results to the loading conditions.
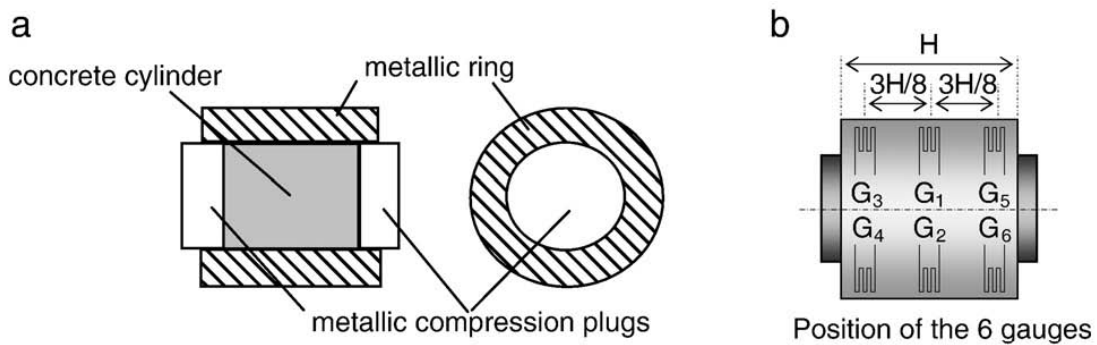
Figure 5.4: Oedometric tests performed by *Forquin et al.* [2010]. Assumptions regarding the confining behavior of the oedometric jacket can be checked with strain gages glues on the jacket. We plan to test such a technique on the crystalline rocks tested in *Doan and D'Hour* [2012] to check the dependance of our results to the loading conditions.

We plan to use the new device to characterize high strain rate behavior of lithologies relevant to fault zones:

– Clays often occur in fault gouges. Mechanically, there behavior is interesting, given their plastic behavior. If they were as sensitive to dynamic loading as crystalline rocks [*Mitchell et al.*, 2013], thermal pressurization could be inhibited.To study such weak rocks, we need to adapt the mini-SHPB to match the low acoustic impedance of clay, by switching to nylon bars.

– Water saturated rocks. We expect fluids to be undrained, inducing local tensile damage near the pores. Previous experiments on saturated concrete showed that water saturation substantially reduces the strength of the rock [*Forquin et al.*, 2010]. We plan to investigate in more detail the case of low porosity crystalline rocks tested by *Doan and D'Hour* [2012], focusing on tensile microstructures expected to be found near pores and fractures.

With the arrival of Pascal Forquin in Grenoble this year, we plan to perform high strain experiments in different loading conditions, rather than uniaxial unconfined loading:

– True onfining experiments, with air confinement (figure 5.2). As SHPB are not servocontrolled, confinement with oil of low compressibility would induce transient large confining pressure. For security reason, we plan to limit the air confinement to 20 MPa, which is small, but enough to go beyond the threshold in confining pressure identified by *Waversik and Brace* [1971] for the disappearing of axial tensile fracturing in low strain rate experiments.

– Dynamic simple shear experiments at the centimetric scale, using a Punch-Through Shear test system mounted on a SHPB device [*Forquin*, 2011] (figure 5.3).

– Controlled oedometric experiments (figure 5.4). The setup designed by Pascal Forquin enables to check a posteriori the assumption on the confining conditions imposed by the jacket (contrary to the experiments of *Yuan et al.* [2011]).

These devices would allow to work on rock deformation at higher confining stress. To go to realistic seismicity conditions, it would be interesting to get higher temperature. However, it is technically difficult to ensure a uniform temperature field within a sample without getting a cumbersome heating device that would complexify the stress field near the sample during dynamic loading. Given these experimental limitations, in-situ observations are the key knowledge to acquire to understand fault mechanics at depth.

5.2.2 Drilling to more seismogenic conditions

Drilling through active fault zones provided a better characterization of the properties of faults down to 2-3 km below surface. This is not deep enough to reach seismogenic conditions, but it enables to understand anomalous behaviors during earthquakes, like the small acceleration recorded during the 1999 Chichi earthquake (TCDP), or the unexpected large slip at the toe of the Tohoku décollement (J-Fast).

Several projects aim at drilling deeper or in hotter environment. In-situ conditions would then favor ductile behavior [*Bürgmann and Dresen*, 2008], either by activation of geochemical processes, like pressure-solution, or by activation of intracrystalline plasticity. Stable creeping becomes more common and at the transition between stable-unstable slip, slow slip events and tremor have be identified [*Rubinstein et al.*, 2010].

I am involved in several projects that could provide information of faults in more ductile environment:

– The second stage of DFDP project aims at drilling at 1500 m. Together with Philippe Pezard, we plan to conduct geophysical logs (especially laterologs), to better characterize the fault properties at depth. With the large heat advected with the uplift of the hanging wall, ductile features, creep are expected to occur.

– The NanTroSEIZE project plans to use riser technology to drill the megasplay fault at $\sim$ 3700 mbsf, and maybe the décollement below 7000 mbsf, by extending the C002 hole. It is currently being drilled down to 3600 mbsf by expedition 348.

– The Japan Beyond Brittle Project aims at testing geothermal energy under ductile conditions, by drilling above a volcanic chamber. It is expected that seismicity generated fluid injections would be dampened by the ductile conditions. I was invited to the preliminary workshop in March 2013. Although the project does not target active faults especially, its discusses important features at hydrofracturing, sliding regimes, and speed of healing.

In all the projects cited above, hydrology is a key parameter. I hope that my expertise exerted in the examples of chapter 4 would be helpful. It would be of special interest to design tools able to stand the long temperature, especially for the long term monitoring. The examples of pore pressure monitoring of chapter 4 reveal that fault environment is quite dynamic, being disturbed by teleseismic waves or preparing a slipping episode. Slow slip events could be preliminary to large earthquakes [*Bouchon et al.*, 2011; *Kato*, 2012]; as they are difficult to monitor from the surface, in-situ monitoring would better understand how faults build before rupture and heal after rupture.

Bibliography

Agnew, D. C. (2007), Earth Tides, in *Treatise on Geophysics: Geodesy*, edited by T. A. Herring, pp. 163–195, Elsevier B.V.

Berryman, K. R., U. a. Cochran, K. J. Clark, G. P. Biasi, R. M. Langridge, and P. Villamor (2012), Major earthquakes occur regularly on an isolated plate boundary fault., *Science (New York, N.Y.)*, *336*(6089), 1690–3, doi:10.1126/science.1218959.

Bhat, H. S., A. J. Rosakis, and C. G. Sammis (2012), A Micromechanics Based Constitutive Model for Brittle Failure at High Strain Rates, *Journal of Applied Mechanics*, *79*(3), 031,016, doi:10.1115/1.4005897.

Bièvre, G., D. Jongmans, T. Winiarski, and V. Zumbo (2011), Application of geophysical measurements for assessing the role of fissures in water infiltration within a clay landslide (Trièves area , French Alps), *Hydrological Processes*, doi:10.1002/hyp.7986.

Bos, B., C. J. Peach, and C. J. Spiers (2000), Frictional-viscous flow of simulated fault gouge caused by the combined effects of phyllosilicates and pressure solution, *Tectonophysics*, *327*(3-4), 173–194.

Bouchon, M., H. Karabulut, M. Aktar, S. Özalaybey, J. Schmittbuhl, and M.-p. Bouin (2011), Extended Nucleation of the 1999, *Science*, *877*, doi:10.1126/science.1197341.

Boutareaud, S., T. Hirose, M. Andréani, M. Pec, D.-G. Calugaru, A.-M. Boullier, and M.-L. Doan (2012), On the role of phyllosilicates on fault lubrication: Insight from micro- and nanostructural investigations on talc friction experiments, *Journal of Geophysical Research*, *117*(B8), B08,408, doi:10.1029/2011JB009006.

Boutt, D. F., D. Saffer, M.-L. Doan, W. Lin, T. Ito, Y. Kano, P. Flemings, L. C. McNeill, T. Byrne, N. W. Hayman, and K. T. Moe (2012), Scale dependence of in-situ permeability measurements in the Nankai accretionary prism: The role of fractures, *Geophysical Research Letters*, *39*(7), 2–7, doi:10.1029/2012GL051216.

Bürgmann, R., and G. Dresen (2008), Rheology of the lower crust and upper mantle: Evidence from rock mechanics, geodesy, and field observations, *Annu. Rev. Earth Planet. Sci.*, doi:10.1146/annurev.earth.36.031207.124326.

Byerlee, J. (1978), Friction of rocks, *Pure and applied Geophysics*, *116*, 615–626.

Caine, J. S., J. P. Evans, and C. B. Forster (1996), Fault zone architecture and permeability structure, *Geology*, *24*(11), 1025–1028.

Candela, T., and F. Renard (2012), Segment linkage process at the origin of slip surface roughness: Evidence from the Dixie Valley fault, *Journal of Structural Geology*, *45*, 87–100, doi:10.1016/j.jsg.2012.06.003.

Carpenter, B. M., C. Marone, and D. M. Saffer (2009), Frictional behavior of materials in the 3D SAFOD volume, *Geophysical Research Letters*, *36*(5), L05,302, doi:10.1029/2008GL036660.

Çakir, Z., S. Ergintav, H. Özener, U. Dogan, A. M. Akoglu, M. Meghraoui, and R. Reilinger (2012), Onset of aseismic creep on major strike-slip faults, *Geology of the Earthquake Source: A Volume in Honour of Rick Sibson*, p. G33522, doi:10.1130/G33522.1.

Chen, W. W., and B. Song (2010), *Split Hopkinson (Kolsky) Bar Design, testing and applications*, Springer Verlag.

Chester, F. M., and J. M. Logan (1986), Implications for mechanical properties of brittle faults from observation of the Punchbowl Fault Zone, California, *Pure and Applied Geophysics*, *124*(1/2), 79–106.

Davis, E. E., K. Wang, K. Becker, and R. E. Thomson (2000), Formation-scale hydraulic and mechanical properties of oceanic crust inferred from pore pressure response to periodic seafloor loading, *Journal of Geophysical Research*, *105*(B6), 13,423—-13,435.

Denoual, C., and F. Hild (2000), A damage model for the dynamic fragmentation of brittle solids, *Computer Methods in Applied Mechanics and Engineering*, *183*, 247–258.

Di Toro, G., R. Han, T. Hirose, N. De Paola, S. Nielsen, K. Mizoguchi, F. Ferri, M. Cocco, and T. Shimamoto (2011), Fault lubrication during earthquakes., *Nature*, *471*(7339), 494–8, doi:10.1038/nature09838.

Doan, M.-L. (2005), Etude in-situ des interactions hydromécaniques entre fluides et failles actives: Application au Laboratoire du Rift de Corinthe, Phd, Institut de Physique du Globe de Paris.

Doan, M.-L., and A. Billi (2011), High strain rate damage of Carrara marble, *Geophysical Research Letters*, *38*(L19302), 1–6, doi:10.1029/2011GL049169.

Doan, M.-L., and F. H. Cornet (2007), Small pressure drop triggered near a fault by small teleseismic waves, *Earth and Planetary Science Letters*, *258*(1-2), 207–218, doi:10.1016/j.epsl.2007.03.036.

Doan, M.-L., and V. D'Hour (2012), Effect of initial damage on rock pulverization along faults, *Journal of Structural Geology*, *45*, 113–124, doi:10.1016/j.jsg.2012.05.006.

Doan, M.-L., and G. Gary (2009), Rock pulverization at high strain rate near the San Andreas fault, *Nature Geoscience*, *2*(10), 709–712, doi:10.1038/ngeo640.

Doan, M.-l., D. Saffer, D. Boutt, and L. Mcneill (a), A full permeability profile of Kumano Forearc Basin, Nankai Trough from modeling of electrical data, *To be submitted to GRL*.

Doan, M.-L., T. Hirose, M. Andréani, A.-m. Boullier, D.-G. Calugaru, and S. Boutareaud (b), Talc Lubrication at High Strain Rate, *to be submitted to J. Struc. Geol.*

Doan, M.-L., E. E. Brodsky, Y. Kano, and K.-F. Ma (2006a), In situ measurement of the hydraulic diffusivity of the active Chelungpu Fault, Taiwan, *Geophysical Research Letters*, *33*(16), 1–5, doi:10.1029/2006GL026889.

Doan, M.-l., E. E. Brodsky, R. Prioul, and C. Signer (2006b), Tidal analysis of borehole pressure : a tutorial, *Tech. rep.*, Schlumberger-Doll Research.

Doan, M.-L., T. M. Mitchell, and G. Gary (2009), Experimental investigation of asymmetric pulverization along the Arima-Takatsuki fault, *Eos Trans. AGU 90(52), Fall Meet. Suppl.*, *90*(52), Abstract T41A–1990, doi:10.1038/ngeo640.

Doan, M.-L., M. Conin, P. Henry, T. Wiersberg, D. F. Boutt, D. Buchs, D. Saffer, L. C. Mcneill, D. Cukur, and W. Lin (2011), Quantification of free gas in the Kumano fore-arc basin detected from borehole physical properties: IODP NanTroSEIZE drilling Site C0009, *Geochemistry Geophysics Geosystems*, *12*(Q0AD06), doi:10.1029/2010GC003284.

Dor, O., T. K. Rockwell, and Y. Ben-Zion (2006), Geological Observations of Damage Asymmetry in the Structure of the San Jacinto, San Andreas and Punchbowl Faults in Southern California: A Possible Indicator for Preferred Rupture Propagation Direction, *Pure and Applied Geophysics*, *163*(2-3), 301–349, doi:10.1007/s00024-005-0023-9.

Dor, O., C. Yildirim, T. K. Rockwell, Y. Ben-Zion, O. Emre, M. Sisk, and T. Y. Duman (2008), Geological and geomorphologic asymmetry across the rupture zones of the 1943 and 1944 earthquakes on the North Anatolian Fault: possible signals for preferred earthquake propagation direction, *Geophysical Journal International*, *173*(2), 483–504, doi:10.1111/j.1365-246X.2008.03709.x.

Dresen, G., M. Bohnhoff, M. Aktar, and H. Eyidogan (2008), Drilling the North Anatolian Fault, *Scientific Drilling*, *6*, 58–59, doi:10.1029/1999.

Dunham, E. M., P. Favreau, and J. M. Carlson (2003), A Supershear Transition mechanism for cracks, *Science*, *299*, 1557–1559.

Faulkner, D. R., A. Lewis, and E. H. Rutter (2003), On the internal structure and mechanics of large strike-slip fault zones: field observations of the Carboneras fault in southeastern Spain, *Tectonophysics*, *367*(3-4), 235–251, doi:10.1016/S0040-1951(03)00134-3.

Faulkner, D. R., T. M. Mitchell, D. Healy, and M. J. Heap (2006), Slip on 'weak' faults by the rotation of regional stress in the fracture damage zone., *Nature*, *444*(7121), 922–5, doi:10.1038/nature05353.

Faulkner, D. R., C. A. L. Jackson, R. J. Lunn, R. W. Schlische, Z. K. Shipton, C. A. J. Wibberley, and M. Withjack (2010), A review of recent developments concerning the structure, mechanics and fluid flow properties of fault zones, *Journal of Structural Geology*, *32*(11), 1557–1575, doi:10.1016/j.jsg.2010.06.009.

Faulkner, D. R., T. M. Mitchell, J. Behnsen, T. Hirose, and T. Shimamoto (2011), Stuck in the mud? Earthquake nucleation and propagation through accretionary forearcs, *Geophysical Research Letters*, *38*(L1830), 1–5, doi:10.1029/2011GL048552.

Forquin, P. (2011), Influence of free water and strain-rate on the shear behaviour of concrete, *Applied Mechanics and Materials*, *82*, 148–153, doi:10.4028/www.scientific.net/AMM.82.148.

Forquin, P., K. Safa, and G. Gary (2010), Influence of free water on the quasi-static and dynamic strength of concrete in confined compression tests, *Cement and Concrete Research*, *40*(2), 321–333, doi:10.1016/j.cemconres.2009.09.024.

Forrestal, M. J., T. W. Wright, and W. W. Chen (2007), The effect of radial inertia on brittle samples during the split Hopkinson pressure bar test, *International Journal of Impact Engineering*, *34*(3), 405–411, doi:10.1016/j.ijimpeng.2005.12.001.

Grady, D. E., and M. E. Kipp (1987), Dynamic rock fragmentation, in *Fracture Mechanics of Rock*, edited by B. K. Atkinson, chap. 10, pp. 429–475, Academic Press Geologic Series.

Gratier, J.-P. (2011), Fault Permeability and Strength Evolution Related to Fracturing and Healing Episodic Processes (Years to Millennia): the Role of Pressure Solution, *Oil Gas Sci. Technol. – Rev. IFP Energies nouvelles*, *66*(3), 491–506, doi:10.2516/ogst/2010014.

Gratier, J.-P., and F. Gueydan (2007), Deformation in the Presence of Fluids and Mineral Reactions Effect of Fracturing and Fluid – Rock Interaction on Seismic Cycles, in *Tectonic Faults: agent of change on a dynamic earth*, edited by M. R. Handy and G. N. Hovius, chap. 12, pp. 319–356, The MIT Press, Cambride, Mass.

Gratier, J.-P., J. Richard, F. Renard, S. Mittempergher, M.-L. Doan, G. Di Toro, J. Hadizadeh, and A.-M. Boullier (2011), Aseismic sliding of active faults by pressure solution creep: Evidence from the San Andreas Fault Observatory at Depth, *Geology*, *39*(12), 1131–1134, doi:10.1130/G32073.1.

Gratier, J.-P., F. Thouvenot, L. Jenatton, A. Tourette, M.-L. Doan, and F. Renard (2013), Geological control of the partitioning between seismic and aseismic sliding behaviours in active faults: Evidence from the Western Alps, France, *Tectonophysics*, *600*, 226–242, doi:10.1016/j.tecto.2013.02.013.

Han, R., T. Shimamoto, T. Hirose, J.-H. Ree, and J.-I. Ando (2010), Ultralow Friction of Carbonate Faults, *Science*, *878*, 878–881, doi:10.1126/science.1139763.

Hild, F., P. Forquin, and A. R. Cordeiro da Silva (2003), Single and multiple fragmentation of brittle geomaterials, *Revue française de génie civil*, *7*(7-8), 973–1002.

Hirose, T. (2005), Growth of molten zone as a mechanism of slip weakening of simulated faults in gabbro during frictional melting, *Journal of Geophysical Research*, *110*(B5), 1–18, doi:10.1029/2004JB003207.

Hsieh, P. A., J. D. Bredehoeft, and J. M. Farr (1987), Determination of aquifer transmissivity from earth tide analysis, *Water Resources Research*, *23*(10), 1824–1832.

Ildefonse, B., D. Blackman, B. John, Y. Ohara, D. Miller, and C. MacLeod (2007), Oceanic core complexes and crustal accretion at slow-spreading ridges, *Geology*, *35*(7), 623, doi:10.1130/G23531A.1.

Ioannides, K. (2003), Soil gas radon: a tool for exploring active fault zones, *Applied Radiation and Isotopes*, *59*(2-3), 205–213, doi:10.1016/S0969-8043(03)00164-7.

Ito, T., A. Funato, W. Lin, M.-l. Doan, D. F. Boutt, Y. Kano, H. Ito, D. Saffer, L. C. Mcneill, T. Byrne, and K. T. Moe (2013), Determination of stress state in deep subsea formation by combination of hydraulic fracturing in situ test and core analysis : A case study in the IODP Expedition 319, *Journal of Geophysical Research*, *118*, 1–13, doi:10.1002/jgrb.50086.

Johnston, M. J. S., R. D. Borcherdt, A. T. Linde, and M. T. Gladwin (2006), Continuous Borehole Strain and Pore Pressure in the Near Field of the 28 September 2004 M 6.0 Parkfield, California, Earthquake: Implications for Nucleation, Fault Response, Earthquake Prediction, and Tremor, *Bulletin of the Seismological Society of America*, *96*(4B), S56–S72, doi:10.1785/0120050822.

Kato, A. (2012), Propagation of Slow Slip Leading Up to the 2011 Mw 9.0 Tohoku-Oki Earthquake, *Science*, *705*, doi:10.1126/science.1215141.

Lin, W., M. L. Doan, J. C. Moore, L. Mcneill, T. B. Byrne, T. Ito, D. Saffer, M. Conin, M. Kinoshita, Y. Sanada, K. T. Moe, E. Araki, H. Tobin, D. Boutt, Y. Kano, N. W. Hayman, P. Flemings, and G. J. Huftile (2010), Present-day principal horizontal stress orientations in the Kumano forearc basin of the southwest Japan subduction zone determined from IODP NanTroSEIZE drilling Site C0009, *Geophysical Research Letters*, *37*(L13303), doi:10.1029/2010GL043158.

Lockner, D. A., C. A. Morrow, D. E. Moore, and S. H. Hickman (2011), Low strength of deep San Andreas fault gouge from SAFOD core., *Nature*, *472*(7341), 82–85, doi:10.1038/nature09927.

Ma, K.-F., H. Tanaka, S.-R. Song, C.-Y. Wang, J.-H. Hung, Y.-B. Tsai, J. Mori, Y.-F. Song, E.-C. Yeh, W. Soh, H. Sone, L.-W. Kuo, and H.-Y. Wu (2006), Slip zone and energetics of a large earthquake from the Taiwan Chelungpu-fault Drilling Project., *Nature*, *444*(7118), 473–6, doi:10.1038/nature05253.

Manga, M., and E. E. Brodsky (2006), SEISMIC TRIGGERING OF ERUPTIONS IN THE FAR FIELD: Volcanoes and Geysers, *Annual Review of Earth and Planetary Sciences*, *34*(1), 263–291, doi:10.1146/annurev.earth.34.031405.125125.

Manga, M., I. Beresnev, E. E. Brodsky, J. E. Elkhoury, D. Elsworth, S. E. Ingebritsen, D. C. Mays, and C.-y. Wang (2012), Changes in permeability caused by transient stresses : field observations, experiments and mechanisms, *Reviews of Geophysics*, *50*, doi:10.1029/2011RG000382.

Manning, C. E. (1995), Phase-equilibrium controls on SiO2 metasomatism by aqueous fluid in subduction zones: Reaction at constant pressure and temperature, *International Geology Review*, *37*(12), 1074–1093.

Melosh, H. J. (1989), Cratering mechanics: contact and compression stage, in *Impact Cratering: A Geologic Process*, chap. 4, pp. 46–59, Oxford University Press.

Mitchell, T. M., and D. R. Faulkner (2009), The nature and origin of off-fault damage surrounding strike-slip fault zones with a wide range of displacements: A field study from the Atacama fault system, northern Chile, *Journal of Structural Geology*, *31*(8), 802–816, doi:10.1016/j.jsg.2009.05.002.

Mitchell, T. M., Y. Ben-Zion, and T. Shimamoto (2011), Pulverized fault rocks and damage asymmetry along the Arima-Takatsuki Tectonic Line , Japan, *Earth and Planetary Science Letters*, *308*(3-4), 284–297, doi:10.1016/j.epsl.2011.04.023.

Mitchell, T. M., M.-l. Doan, H. S. Bhat, J. Renner, and G. Girty (2013), High permeabilities in the damage zone of the San Jacinto Fault induced by earthquake rupture.

Moe, K. T., T. Ito, W. Lin, M.-l. Doan, D. Boutt, Y. Kawamura, C. K. Khong, L. Mcneill, T. Byrne, D. Saffer, E. Araki, N. Eguchi, I. Sawada, P. Flemings, Y. Kano, C. Moore, M. Kinoshita, and H. J. Tobin (2012), Operational Review of the First Wireline In Situ Stress Test in Scientific Ocean Drilling, *Scientific Drilling*, *13*, 35–39, doi:10.2204/iodp.sd.13.06.2011.

Moore, D. E., and D. A. Lockner (2011), Frictional strengths of talc-serpentine and talc-quartz mixtures, *Journal of Geophysical Research*, *116*(B1), doi:10.1029/2010JB007881.

Moore, D. E., and M. J. Rymer (2007), Talc-bearing serpentinite and the creeping section of the San Andreas fault, *Nature*, *448*, 795–797, doi:10.1038/nature06064.

Niemeijer, A., C. Marone, and D. Elsworth (2010), Fabric induced weakness of tectonic faults, *Geophysical Research Letters*, *37*(L03304), doi:10.1029/2009GL041689.

Paterson, M. S., and T.-F. Wong (2005), *Experimental rock deformation–the brittle field*, Springer Verlag.

Rempe, M., T. Mitchell, J. Renner, S. Nippress, Y. Ben-Zion, and T. Rockwell (2013), Damage and seismic velocity structure of pulverized rocks near the San Andreas Fault, *Journal of Geophysical Research: Solid Earth*, *118*(6), 2813–2831, doi:10.1002/jgrb.50184.

Rice, J. R. (1992), Fault stress states, pore pressure distributions, and the weakness of the San Andreas fault, in *Fault mechanics and transport properties of rocks*, edited by B. Evans and T.-f. Wong, internatio ed., chap. 20, pp. 475–503, Academic Press Ltd.

Richard, J., J.-P. Gratier, M.-L. Doan, A.-M. Boullier, and F. Renard (2014a), Time and space evolution of an active creeping fault zone: insights from the brittle and ductile microstructures in the San Andreas Fault Observatory at Depth, *To be submitted to JGR*.

Richard, J., M.-L. Doan, J.-P. Gratier, F. Renard, and A.-M. Boullier (2014b), Microstructures of dynamic damaging and healing by fluid circulations into a porous limestone 3, *In preparation*.

Rubinstein, J. L., D. R. Shelly, and W. L. Ellsworth (2010), Non-volcanic tremor: A window into the Roots of Fault Zones, in *New frontiers in Integrated Solid Earth Sciences*, edited by S. Cloetingh and J. Negendank, pp. 287–314, Springer Netherlands, Dordrecht, doi:10.1007/978-90-481-2737-5.

Saffer, D. M., P. B. Flemings, D. F. Boutt, M.-L. Doan, T. Ito, L. C. Mcneill, T. B. Byrne, M. Conin, W. Lin, E. Araki, N. Eguchi, S. Toczko, and Y. Kano (2013), In situ stress and pore pressure in the Kumano Forearc Basin, offshore SW Honshu from downhole measurements during riser drilling, *Geochemistry, Geophysics, Geosystems*, *14*(5), doi:10.1002/ggge.20051.

Shi, Z., and Y. Ben-Zion (2006), Dynamic rupture on a bimaterial interface governed by slip-weakening friction, *Geophysical Journal International*, *165*(2), 469–484, doi:10.1111/j.1365-246X.2006.02853.x.

Sibson, R. H. (1992), Implication of fault-valve behaviour for rupture nucleation and recurrence, *Tectonophysics*, *211*, 283–293.

Spencer, J. Q., J. Hadizadeh, J.-P. Gratier, and M.-L. Doan (2012), Dating deep? Luminescence studies of fault gouge from the San Andreas Fault zone 2.6 km beneath Earth's surface, *Quaternary Geochronology*, *10*, 280–284, doi:10.1016/j.quageo.2012.04.023.

Sutherland, R., V. G. Toy, J. Townend, S. C. Cox, J. D. Eccles, D. R. Faulkner, D. J. Prior, R. J. Norris, E. Mariani, C. Boulton, B. M. Carpenter, C. D. Menzies, T. A. Little, M. Hasting, G. P. De Pascale, R. M. Langridge, H. R. Scott, Z. Reid Lindroos, B. Fleming, and A. J. Kopf (2012), Drilling reveals fl uid control on architecture and rupture of the Alpine fault , New Zealand, *Geology*, pp. 1–4, doi: 10.1130/G33614.1.

Tary, J.-B., L. Géli, C. Guennou, P. Henry, N. Sultan, N. Çağatay, and V. Vidal (2012), Microevents produced by gas migration and expulsion at the seabed : a study based on sea bottom recordings from the Sea of Marmara, *Geophysical Journal International*, *190*, 993–1007, doi:10.1111/j.1365-246X.2012.05533.x.

Tobin, H. J., and M. Kinoshita (2006), NanTroSEIZE: The IODP Nankai Trough Seismogenic Zone Experiment, *Scientific Drilling*, *2*, 23–27, doi:10.2204/iodp.sd.2.06.2006.

Wang, K., and E. E. Davis (1996), Theory for the propagation of tidally induced pore pressure variations in layered subseafloor formations, *J. Geophys. Res.*, *101*(B5), 11,483–11,495.

Waversik, W. R., and W. F. Brace (1971), Post-Failure Behavior of a Granite and Diabase, *Rock Mechanics*, *3*(2), 61–85.

Weibull, W. (1939), A statistical theory of the strength of materials, *Ingeniörsvetenskapsakademiens handlingar*, *151*, 1–4.

Wibberley, C. a. J., and T. Shimamoto (2005), Earthquake slip weakening and asperities explained by thermal pressurization., *Nature*, *436*(7051), 689–92, doi:10.1038/nature03901.

Wiersberg, T., and J. Erzinger (2008), Origin and spatial distribution of gas at seismogenic depths of the San Andreas Fault from drill-mud gas analysis, *Applied Geochemistry*, *23*(6), 1675–1690, doi:10.1016/j.apgeochem.2008.01.012.

Wilson, B., T. A. Dewers, Z. Reches, and J. N. Brune (2005), Particle size and energetics of gouge from earthquake rupture zones Brent, *Nature*, *434*, 749—-752, doi:10.1029/2003GL019277.

Yuan, F., V. Prakash, and T. E. Tullis (2011), Origin of pulverized rocks during earthquake fault rupture, *Journal of Geophysical Research*, *116*(B6), 1–18, doi:10.1029/2010JB007721.

Zoback, M., S. Hickman, and W. Ellsworth (2011), Scientific drilling into the San Andreas Fault Zone - An overview of SAFOD's first five years, *Scientific Drilling*, doi:10.2204/iodp.sd.11.02.2011.

Appendix A

Curriculum Vitae

A.1   Education / Professional cursus

2007-... Assistant Professor at University Joseph Fourier, Grenoble, France

2006-2007 Postdoctoral researcher at the University of California, Santa Cruz (UCSC) with Emily BRODSKY.

End 2005 Postdoctoral researcher at the University of California, Los Angeles (UCLA) with Emily BRODSKY.

2000-2005 PhD, Institut de Physique du Globe de Paris.
Titre:
***in-situ* study of the hydromechanical interactions between fluids and active faults**
5 juillet 2005
PhD commitee:

Claude	JAUPART	Institut de Physique du Globe de Paris	President
Philippe	DAVY	Université de Rennes I	Rapporteur
Pierre	HENRY	Collège de France, Aix-en-Provence	Rapporteur
Ghislain	DE MARSILY	Université de Paris VI	Examinateur
Ian	MAIN	Edimburgh University	Examinateur
François	CORNET	Institut de Physique du Globe de Paris	PhD Advisor

2001 "Agrégation" of Physics

2000 Magistère Interuniversitaire de Physique, Ecole normale supérieure-Paris

A.2   Committee memberships and awards

– 2010-2011: Member of the Engineering Development Panel (EDP) of the Integrated Oceanic Drilling Program (IODP)

– 2010-2011: Member of the Conseil National des Universités (CNU / French committee)

– 2009 Best reviewer award, Geophysical Journal International

– Invited speaker at several conferences (EGU, ICDP/IODP meetings)

A.3   Collaborations

A.3.1   Pulverization

Experimental development Gérard Gary (Ecole polytechnique), Pascal Forquin (LEM3, Metz, now in Grenoble University), Jean-Pierre Gratier (Grenoble University), Frans Aben (Grenoble University)

Microstructures Tom Mitchell (now in University College London), Julie Richard (ISTerre), Andrea Billi (Consiglio Nazionale delle Ricerche, Italy), Michele Fondriest (Padova University), Joel Spencer (Kansas State University), Mike Heap (Strasbourg University), Ulrich Kueppers (Ludwig-Maximilians-Universität, Munich).

A.3.2 High velocity friction experiments

Experimental development Takehiro Hirose (JAMSTEC, Japan) that was an invited researcher in Grenoble

Microstructures Muriel Andréani (Lyon University), Anne-Marie Boullier (ISTerre), Sébastien Boutareaud (ETH Zürich, now at EuroEngineering, Pau) and Dan-Gabriel Calugaru (Institut Néel, Grenoble)

A.3.3 Drilling projects

TCDP Kuo-Fong Ma (NCU, Taiwan), Emily Brodsky (UC Santa Cruz), Yasuyuki Kano (Kyoto University)

NanTroSEIZE Pierre Henry (CEREGE), Marianne Conin (CEREGE, now Guadelupe University), Demian Saffer (PennState), David Boutt (Massachusetts University), Weiren Lin (JAMSTEC, Japan), Thomas Wiersberg (GFZ Postdam)

DFDP Rupert Sutherland (GNS), John Townend (Victoria University of Wellington), Philippe Pezard (Montpellier University)

Avignonet Grégory Bièvre (ISTerre), Denis Jongmans (ISTerre)

A.4 Supervision of students

A.4.1 PhD Students

Julie Richard (2010-2013) This PhD thesis is co-supervised together with Jean-Pierre Gratier on "Creeping mechanisms in active faults: lessons from international drilling projects". During this PhD, Julie combined microstructural studies of cores samples in SAFOD borehole together with experiments on healing of samples damages experimentally at high strain rate. During this PhD, Julie was invited to take initiatives, to meet and interact with researchers as often as possible (eg, by chairing sessions during international meetings). She will finish her PhD with 3 publications [*Gratier et al.*, 2011; *Richard et al.*, 2014a,b]

Frans Aben (2013-2016) This PhD thesis is co-supervised together with François Renard on "Creating and clogging dynamic permeability in fault zones and geological reservoirs", funded through the FlowTrans Initial Training Network, funded by the EU. This PhD is the continuation of the PhD of Julie Richard, with more stress put on the experiments. With Frans, we plan to work on dynamic damage and by improving the instrumentation of percolation cells by adding a cell for measuring permeability.

A.4.2 Supervision of research internships

I supervised several interns from the Master of Grenoble University

Camille Litty (2012) We investigated X-ray CT scans of samples almost "pulverized"from a Himalayan Fault sampled by Anne Replumaz (ISTerre).

Virginie d'Hour (2009) We performed together high strain rate experiments on analog of intact granite, compared to damaged samples of the San Andreas Fault [*Doan and D'Hour*, 2012]

Alexandre Tourette (2008) We conducted field work on the structure of the Clery Fault, comparing strain localization in shales and limestone [*Gratier et al.*, 2013].

Appendix B

Publications

B.1   Publication list

1. Gratier, J-P., Thouvenot, F., Jenatton, L., Tourette, A., **Doan, M.L.** and Renard, F. Geological control of the partitioning between seismic and aseismic sliding behaviour in active faults : evidence from the Western Alpes, France.,*Tectonophysics*, 600:226-242, doi:10.1016/j.tecto.2013.02.013, 2013

2. Ito, T., Funato , A., Lin, W., **Doan, M.L.**, Boutt, D., Kano , Y. Ito , H., Saffer, D. McNeill, L., Byrne, T,Moe, K. Determination of Stress State in Deep Subsea Formation by Combination of Hydraulic Fracturing In-situ Test and Core Analysis - A Case Study in the IODP Expedition 319, *J. Geophys. Res.*, 118, 1–13, doi:10.1002/jgrb.50086, 2013

3. Saffer, D., Flemings, P., Boutt, D., **Doan, M.L.**, Ito, T., McNeill, L., Byrne, T., Conin, M.,Lin, W., Kano, Y., Araki, E., Eguchi N., Toczko, S.. In Situ Stress and Pore Pressure in the Kumano Forearc Basin, offshore SW Honshu from Down-hole Measurements During Riser Drilling, *Geophys. Geochem. Geosystems*, 14(5), doi:10.1002/ggge.20051, 2013

4. Moe, K.T., Ito, T., Lin, W., **Doan, M.L.**, Boutt, D., Kawamura, Y., Khong, C.K. McNeill, L., Byrne, T., Saffer, D., Araki, E., Eguchi, N., Sawada, I., Flemings, P., Kano, Y. Moore, C., Kinoshita, M., Tobin, H. Operational Review of the First Wireline in Situ Stress Test in Scientific Ocean Drilling, *Scientific Drilling*, 13:35-39, 2012

5. Boutareaud, S., Hirose, , T. Andréani, M., Pec, M., Kunze, K., Calugaru, D.-G.,. Boullier, A.-M., **M.-L. Doan**. On the role of phyllosilicates on fault lubrication: Insight from micro- and nanostructural investigations on talc friction experiments, *J. Geophys. Res*, 117 (B8), B08408, doi: 10.1029/2011JB009006, 2012

6. **Doan, M.L.** and V. d'Hour, Effect of initial damage on rock pulverization along faults, *J. Struct. Geol.*, 45:113-124, 2012

7. Spencer, J.Q.G., Hadizadeh, J., Gratier, J.-P. and **M-L Doan**, Dating deep? Luminescence studies of fault gouge from the San Andreas Fault Zone 2.6 km beneath Earth's surface, *Quat. Geochronol.*, 10: 280-284, 2012

8. Boutt, D., D. Saffer, **M.-L. Doan**, W. Lin, T. Ito, Y. Kano, P. Flemings, L. McNeil, T. Byrne, K. Moe. Scale Dependence of In-situ Permeability Measurements in the Nankai Accretionary Prism: The Role of Fractures, *Geol. Res. Lett.*, 39, L07302, doi:10.1029/2012GL051216, 2012

9. **Doan, M.L.**, and A. Billi, [High strain rate damage of Carrara marble, *Geophys. Res. Lett.*, 38, L19302, doi:10.1029/2011GL049169, 2011

10. Gratier, J-P., J. Richard, Renard, F., S. Mittempergher, **Doan, M.L.**, G. Di Toro, J. Hadizadeh and A-M. Boullier. Aseismic sliding of active faults by pressure solution creep: Evidence from the San Andreas Fault Observatory at Depth (SAFOD). *Geology*, 39, 1131-1134, 2011

11. **Doan, M.L.**, Conin, M., Henry, P., Wiersberg, T., Boutt, D., Buchs, D.,Saffer, D., McNeill, L., Cukur. Free gas in Kumano basin detected from borehole sonic data in IODP NanTroSEIZE drilling Site C0009, *Geophys. Geosystems Geochem*, 12: doi:10.1029/2010GC003284, 2011

12. Lin, W., **Doan, M.L.**, Moore, J.C., McNeill, L., Byrne, T.B., Ito, T., Saffer, D., Conin, M., Kinoshita, M., Sanada, Y., Moe, K.T., Araki, E., Tobin, H., Boutt, D., Kano, Y., Hayman, N.W., Flemings, P., Huftile,G. J., Cukur, D., Buret, C., Schleicher, A.M., Efimenko, N., Kawabata, K., Buchs, D.M., Jiang, S., Kameo, K., Horiguchi, K., Wiersberg, T., Kopf, A., Kitada, K., Eguchi, N., Toczko, S., Takahashi, K. and Kido, Y., Present-day principal horizontal stress orientations in the Kumano forearc basin of the southwest Japan subduction zone determined from IODP NanTroSEIZE drilling Site C0009, *Geophys. Res. Lett.*, 37, L13303, doi:10.1029/2010GL043158, 2010.

13. Noiriel C., Renard, F., **Doan, M.L.**, and J.-P. Gratier. Intense fracturing and fracture sealing induced by mineral growth in porous rocks. *Chem. Geol.*, 269(3-4):197-209, 2010

14. **Doan, M.L.** and G. Gary., Rock pulverization at high strain rate near the San Andreas Fault, *Nature Geoscience*, 2: 709-712, 2009

15. **Doan, M.L.** and F.H. Cornet. Small pressure drop triggered near a fault by small teleseismic waves. *Earth Planet. Sci. Lett.*,258 (1-2): 207-218, 2007

16. **Doan, M.L.** and F.H. Cornet. Thermal Convection below the Aigio Fault, Gulf of Corinth, Greece. *Geophys. Res. Lett.*, 34 (6) doi:10.1016/j.epsl.2007.03.036, 2007

17. **Doan, M.L.**, E.E. Brodsky, Y. Kano, and K.-F. Ma, In situ measurement of the hydraulic diffusivity of the active Chelungpu Fault, Taiwan. *Geophys. Res. Lett.*, 33 (16) doi:10.1029/2006GL026889, 2006.

18. F.H. Cornet, **M.L. Doan**, I. Moretti and G. Borm. Drilling through the active Aigion fault : the AIG10 well observatory. *C.R. Géoscience*, 2004.

19. F.H. Cornet, **M.L. Doan**, and F. Fontbonne. Electrical imaging and hydraulic testing for a complete stress determination. *Int. J. Rock Mech. Min. Sci.*, 40 :1225-1241, 2003.

20. **Doan, M.L.** and F.H. Cornet. A coupled hydraulic and electrical stress determination technique. In Hammah R. et al, editor, *Mining and Tunneling Innovation and Opportunity*, volume 2, page 1413. NARMS-TAC, University of Toronto Press, 2002.

B.2 Papers in preparation

1. **Doan, M.L.** , Hirose, T., Andréani, M. Boullier, A.-M., Calugaru, D.-G., Boutareaud, S. Talc lubrication at high strain rate. To be submitted to J. Struct. Geol.

2. **Doan, M.L.** , Saffer, D., Boutt, D., and Mcneill, L. A full permeability profile of Kumano Forearc Basin, Nankai Trough from modeling of electrical data. To be submitted to Geophys. Res. Lett.

3. Mitchell, T.M.,**Doan, M.L.** ., Bhat, H.S., Renner, J., and Girty, G. High permeabilities in the damage zone of the San Jacinto Fault induced by earthquake rupture: To be submitted to Science

4. Richard, J., Gratier, J.-P., **Doan, M.L.** ., Boullier, A.-M., and Renard, F., Time and space evolution of an active creeping fault zone: insights from the brittle and ductile microstructures in the San Andreas Fault Observatory at Depth. To be submitted to J. Geophys. Res.

5. Richard, J., **Doan, M.L.** , Gratier, J.-P., Renard, F., and Boullier, A.-M., Microstructures of dynamic damaging and healing by fluid circulations into a porous limestone. In prep.

Appendix C

A selection of papers

I introduce some selected papers that are collected afterwards, by summarizing them in 2 sentences or less.

C.1   High velocity experiments with talc

Boutareaud et al, J. Geophys. Res., 2012 High velocity friction experiments on talc, with unexpected high friction coefficient for dry talc. Microstructures show nanoagregates of delaminated talc.

Doan et al, to be submitted to J. Struct. Geol. Little amount of talc (5%) is enough to level off the initial peak in friction of a serpentine gouge. It alters also microstructure by creating myriads of small shear planes along the delaminating talc platelets

C.2   High strain rate damage

Doan and Gary, Nature Geoscience, 2009 Samples of the San Andreas Fault are multifragmented when loaded with strain rate larger than 150/s, suggesting that pulverized rocks are product of supershear earthquakes.

Doan and Billi, Geophys. Res. Lett., 2009 High strain rate damage experiments on marble. Damage is controlled by strain rather than by strain rate

Doan and d'Hour, J. Struct. Geol., 2012 High strain rate damage experiments on sound granite, where pulverization could be reproduced but with a larger strain rate threshold.

Gratier et al, Geology, 2011 Extensive pressure solution is found within the SAFOD sample. This process intensity is compatible with the current creep rate of the San Andreas Fault, thanks to intense microfracturing of gouge grains.

Richard et al, to be submitted to J. Geophys. Res. Microstructural studies of the SAFOD sample with data from the saponite gouge and the surrounding material. We discuss the competition between weak friction and pressure solution.

C.3   Borehole geophysics

Doan et al, Geophys. Res. Lett., 2006 Cross-hole experiments across the Chelungpu Fault, through the damage zone bording the strand at the origin of the 1999 Chichi earthquake.

Doan et al, Earth. Planet. Sci. Lett., 2007 Long term monitoring within the Aigio Faut (Greece), with hydraulic anomaly triggered by teleseismic waves.

Lin et al., Geophys. Res. Lett., 2009 Use of data of the Formation Microseismic Imager data to get the orientation of the principal stress directions, in the C009 borehole drilled in the Nankai subduction zone during IODP expedition 319.

Doan et al., Geochem. Geophys. Geosyst., 2011 Use of sonic data to derive a full profile of porosity and gas content in the C009 borehole

Doan et al., to be submitted to Geophys. Res. Lett. Use of electrical data affected by the invasion of the formation by borehole fluids, to derive continuous profile of permeability within the C009 borehole.